AEC RESEARCH AND DEVELOPMENT REPORT

HW-71500 A

MASTER

THE H-3 IRRADIATION EXPERIMENT: IRRADIATION OF EGCR GRAPHITE

INTERIM REPORT NO. 1

J. M. DAVIDSON and J. W. HELM

OCTOBER 16, 1961

HANFORD LABORATORIES

HANFORD ATOMIC PRODUCTS OPERATION
RICHLAND, WASHINGTON

GENERAL ELECTRIC

HW-71500 A

UC-25, Metals, Ceramics
and Materials
(TID-4500, 16th Ed.)

THE H-3 IRRADIATION EXPERIMENT: IRRADIATION OF EGCR GRAPHITE INTERIM REPORT NO. 1

By

J. M. Davidson and J. W. Helm

Materials Development
Reactor and Fuels Research and Development
Hanford Laboratories Operation

October 16, 1961

HANFORD ATOMIC PRODUCTS OPERATION
RICHLAND, WASHINGTON

Work performed under Contract No. AT(45-1)-1350 between the
Atomic Energy Commission and General Electric Company

Printed by/for the U. S. Atomic Energy Commission

Printed in USA. Price $1.75. Available from the
Office of Technical Services
Department of Commerce
Washington 25, D. C.

DISCLAIMER

TABLE OF CONTENTS

THE H-3 IRRADIATION EXPERIMENT: IRRADIATION OF EGCR GRAPHITE - INTERIM REPORT NO. 1

INTRODUCTION

The Experimental Gas-Cooled Reactor (EGCR) is a graphite-moderated reactor utilizing massive graphite bars, approximately 16 inches square and 20 feet long, placed vertically and assembled into a structure approximately 16 feet in diameter.

Nonuniform flux intensity through the massive EGCR graphite bars will result in differential distortion and associated stress gradients. During the lifetime of the EGCR, stress concentrations sufficient to rupture some of the graphite bars may be attained. Assessment of the potential problems of stress fracture and bowing of the monolithic columns depends on a knowledge of the amount of radiation damage to graphite. Damage is dependent on the type of graphite, the temperature of irradiation, and the neutron exposure.

Much information obtained previously at Hanford was useful in design of the EGCR, but it did not fulfill the exact requirements for predicting gross behavior of the moderator during the lifetime of the EGCR. To develop satisfactory data for this purpose, a series of irradiation experiments, designated H-3, was started in the General Electric Test Reactor (GETR). Two irradiation periods have been accomplished to date and this report presents the results. The irradiation capsules were designated H-3-1 and H-3-2.

SUMMARY

Irradiation experiments are being performed in the GETR to determine the long-term stability of EGCR graphite. The results of two experiments with a peak total exposure equivalent to 38,000 MWD/AT in the EGCR are now available. This is approximately one half the expected lifetime exposure of the EGCR.

The H-3-1 and H-3-2 capsules contained samples of EGCR graphite and reference CSF graphite. Both capsules were identical and were irradiated sequentially to increase the dose on the samples. Sixty per cent of the samples irradiated in the H-3-1 capsule were reirradiated in the H-3-2 capsule.

The capsule design utilized the gamma heating of the GETR E-7 facility to achieve desired operating temperatures. The temperatures on inter- and intra-cycle irradiation were constant within 25 C. Samples were irradiated in a temperature range of 475 to 850 C.

The graphite tested was obtained from a full-size cross section of an EGCR block. Irradiation results did not indicate differences in contraction of parallel samples chosen at several positions within the block. Contraction rates of the graphites tested were found to depend on the temperature of irradiation. Estimates of the contraction rates of parallel samples of EGCR graphite are 0.15 per cent per 10^{21} nvt at 575 C and 0.19 per cent per 10^{21} nvt at 475 C (See pages 23 and 39). Parallel samples contracted at a higher rate than the transverse samples. The observed length changes are presented as a function of exposure in Figures 10 through 13.

DESIGN AND CONSTRUCTION OF EXPERIMENT

Sample Selection and Preparation

At the time of construction of the H-3-1 capsule, actual EGCR graphite was not available. However, a graphite electrode, produced from raw materials and manufactured by processes similar to those specified for EGCR bars, was supplied by the National Carbon Company. The bar (designated NC-7) was 16 inches square in cross section, which compares favorably with specifications for the EGCR extrusion. This bar furnished all of the EGCR-type graphite for the H-3-1 capsule. For the H-3-2 capsule, a broken bar of EGCR graphite (designated NC-8) was available and a partial change to actual EGCR material was made. In order to gain high exposure data rapidly some NC-7 graphite from the H-3-1 capsule was included in H-3-2. The graphite samples irradiated are described in Table I.

TABLE I

GRAPHITE DESCRIPTION

Hanford Designation	Supplier	Coke Source and Type	Extrusion Size (Inches)	Remarks
CSF - BAAD	National Carbon Company	Cleves, conventional	4 x 4 x 50	Reactor grade; F-purified at 2700 C; density: 1.66 g/cc
NC-7 - AAAD	National Carbon Company	Continental-Lake Charles, Needle	16-3/8 x 16-3/8 x 4-1/4	Electrode stock; similar to graphite used for EGCR; density: 1.70 g/cc
NC-8 - AAAD	National Carbon Company	Continental-Lake Charles, Needle	17-1/2 x 17-1/2 x 10	Reactor grade: AGOT; EGCR graphite; density: 1.72 g/cc

Artificial graphite that is extruded during manufacture is known to show some secondary orientation effects of the shaping die. This anisotropy, while less than the parallel-to-transverse* anisotropy, is detectable by X-ray and eddy-current measurements. Eddy-current measurements of the NC-7 bar showed that the crystallite orientation at the edge (measurement made on a transverse face) was preferentially parallel to the edge, while the crystallite orientation at the center was random. Because anisotropy of this sort may influence radiation-induced contraction, it was considered desirable to test samples from several places in the large

* Graphite extrusions generally are longer in the dimension parallel with the axis of extrusion than in the direction perpendicular to extrusion. The extrusion process causes pronounced differences in the physical properties of the two directions. Obviously, the terms "parallel" or "longitudinal", and "perpendicular" or "transverse" have no real significance except when referring to the extrusion process; they become more troublesome if molded graphite is considered. The terms "with the grain" and "against the grain" are perhaps better but they, too, are limited descriptively. This report uses the arbitrarily selected terms "parallel" ($\parallel$) and "transverse" ($\perp$) to mean directions with respect to the extrusion axis.

extrusions. Samples designated N-1, N-2, and N-3 (Figure 1) were taken at the center, midpoint, and edge of the bar. NC-8 samples at the same locations were designated P-1, P-2, and P-3. Figure 2 shows the locations from which the CSF samples were obtained.

After machining to a quarter-round shape, the individual samples were annealed at 1900 C for 45 minutes at a pressure of 5×10^{-4} mm of mercury to remove a small, thermally annealable strain present in fabricated samples.[1] Lengths were measured optically and physically on all samples prior to irradiation. A Bausch and Lomb DR-25 Optical Gage (Type 33-14-23) was used for physical end-to-end measurements, and a Bausch and Lomb Bench Comparator (Type 33-12-11) was used for measurements of the distances between spaced holes drilled in the samples. These devices, when used to measure graphite, have a standard deviation of 2×10^{-5} and 15×10^{-5} inches, respectively.

Capsule Design

Two capsules, designated H-3-1 and H-3-2, were constructed and have been irradiated. They were basically of similar design and, except as noted hereafter, can be considered identical. Substantial features from the design of the H-1 Experiment[2] were used in the design of the H-3 capsule series. The desired operating temperature of the samples in capsules of the H-1 type is achieved by utilizing the gamma heating of the samples with specially designed heat loss paths to the reactor coolant. Basic changes in mounting configurations were made to cause lower operating temperatures in the H-3 capsules. The capsule heat transfer properties were computed (Appendix A) and the design was checked by laboratory simulation of reactor conditions on a prototype capsule before fabrication and irradiation of the H-3-1 capsule.

Figures 3 and 4 show internal views of the H-3-1 capsule. The H-3-2 capsule differed in that 15 highly radioactive samples from the first capsule were built into the sample string. This necessitated special handling and generally made construction more difficult. The samples

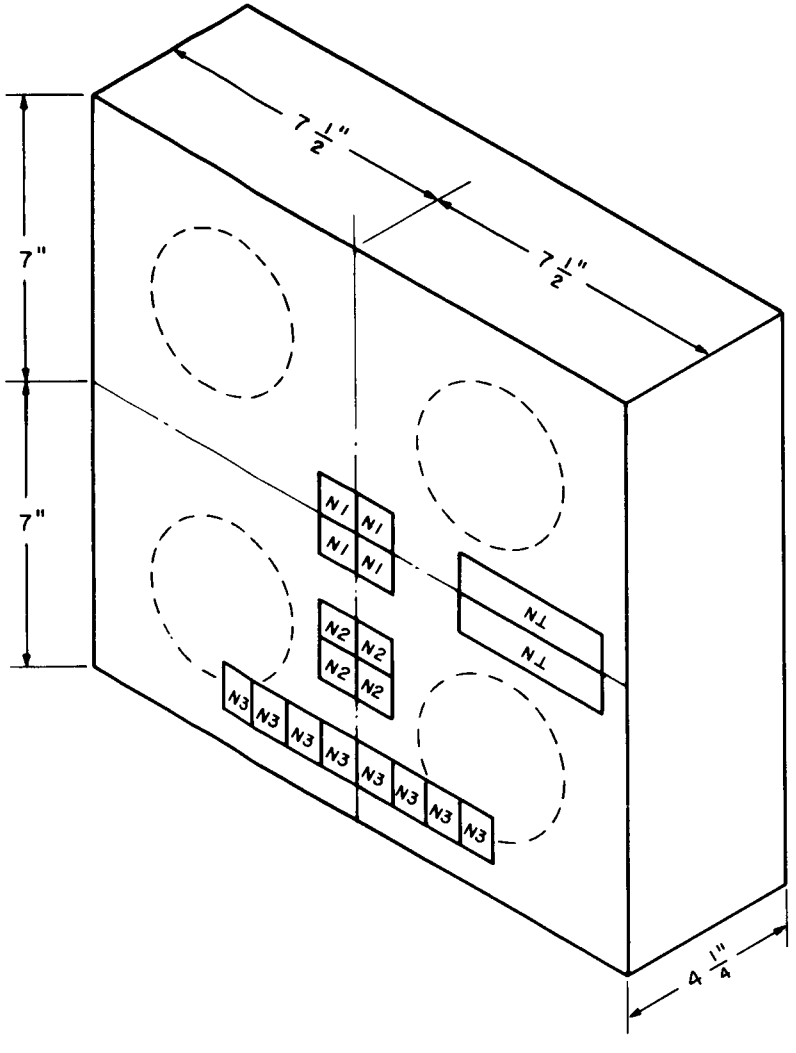

Legend

1. NC-7 Graphite
   - N1 Parallel
   - N2 Parallel
   - N3 Parallel
   - NT Transverse
2. NC-8 Graphite
   Same as Above, Numbered P
3. Dashed Circles in Position of EGCR Fuel Channels

FIGURE 1

Sampling Scheme
Needle Coke Graphites

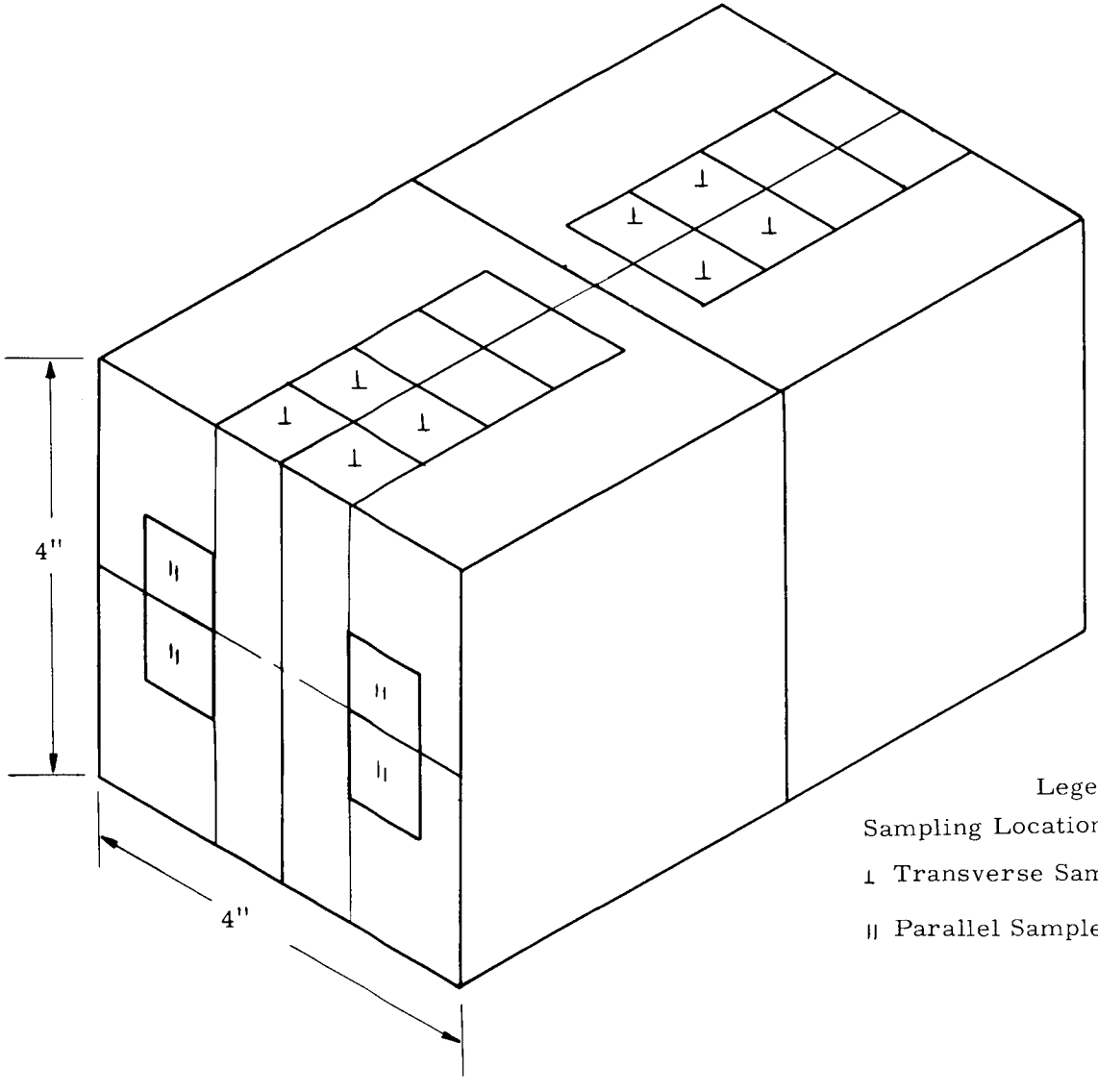

FIGURE 2

Sampling Scheme
CSF Reference Graphite

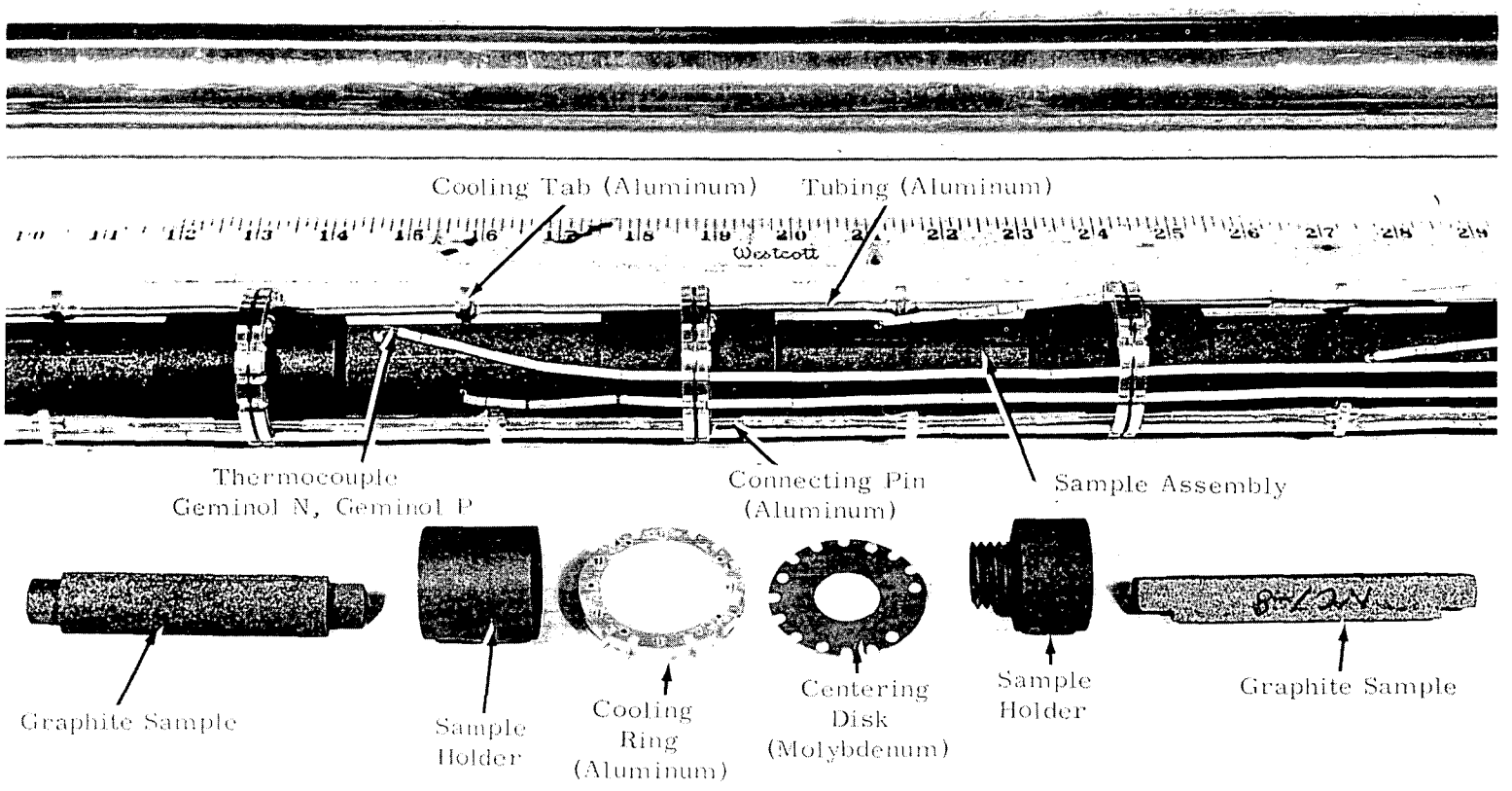

FIGURE 3

Internal View
H-3 Capsule Series

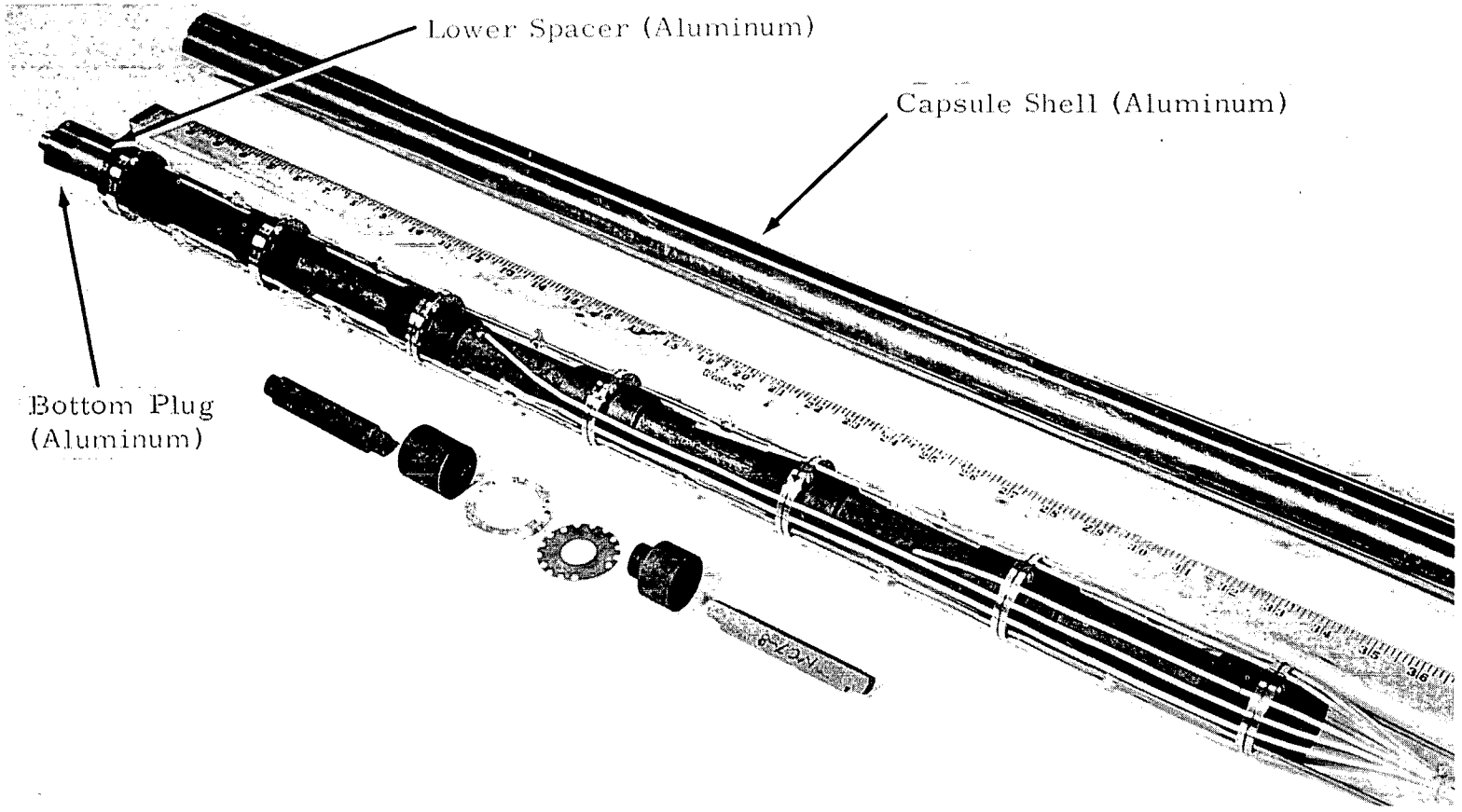

FIGURE 4

Internal View
H-3 Capsule Series

were assembled four in a group: three samples of EGCR material and one CSF reference sample. Six groups were included in the capsule. The groups were mounted axially in the capsule and held together by graphite holders designed to accommodate thermal expansion. Each set of holders was screwed together through holes in transversely oriented 0.030-inch thick molybdenum disks which limited heat flow to aluminum cooling rings. The cooling rings were spaced by aluminum tubes. To cool the connecting tubes adequately, tabs were located at mid-run positions to thermally ground the tubes to the cool capsule shell. Geminol N-P thermocouples were attached to each sample group to monitor temperatures of irradiation. Fast and thermal neutron flux monitors were installed in the cooling rings to facilitate determination of neutron exposure. After subassembly, as shown in Figures 3 and 4, the capsule shell was installed and compressed (by swaging) onto the cooling rings to obtain reproducible thermal contact.

Upper and lower end plugs were welded to the capsule shell. The upper end plug attached to a tube containing the thermocouple wires which were terminated in a primary seal. The seal is shown in Figure 5. The primary seal was made by a Deutsch DM-5605 hermetic receptacle. The receptacle and attached plug were protected with a seal cover. All space between the cover and the receptacle was filled with General Electric No. RTV-60 silicone rubber.

The capsule was carefully leak checked and filled with purified helium. The capsule was pressurized to 80 psig with helium through the evacuation tube in the lower plug and a helium leak detector was used to check the external capsule, tube, and lead termination surfaces. The capsule then was attached to a vacuum system and evacuated to 0.2 mm of mercury for 16 hours. During evacuation, the capsule was heated to approximately 400 C to facilitate outgassing. With the leak detector connected to the vacuum system, a second helium leak check was made by blowing helium on the evacuated capsule. The capsule, after determination of its integrity, was filled to a pressure of 770 mm of mercury with de-oxygenated helium which had passed through a liquid nitrogen cold trap. The evacuation tube was crimped shut, cut off, and welded.

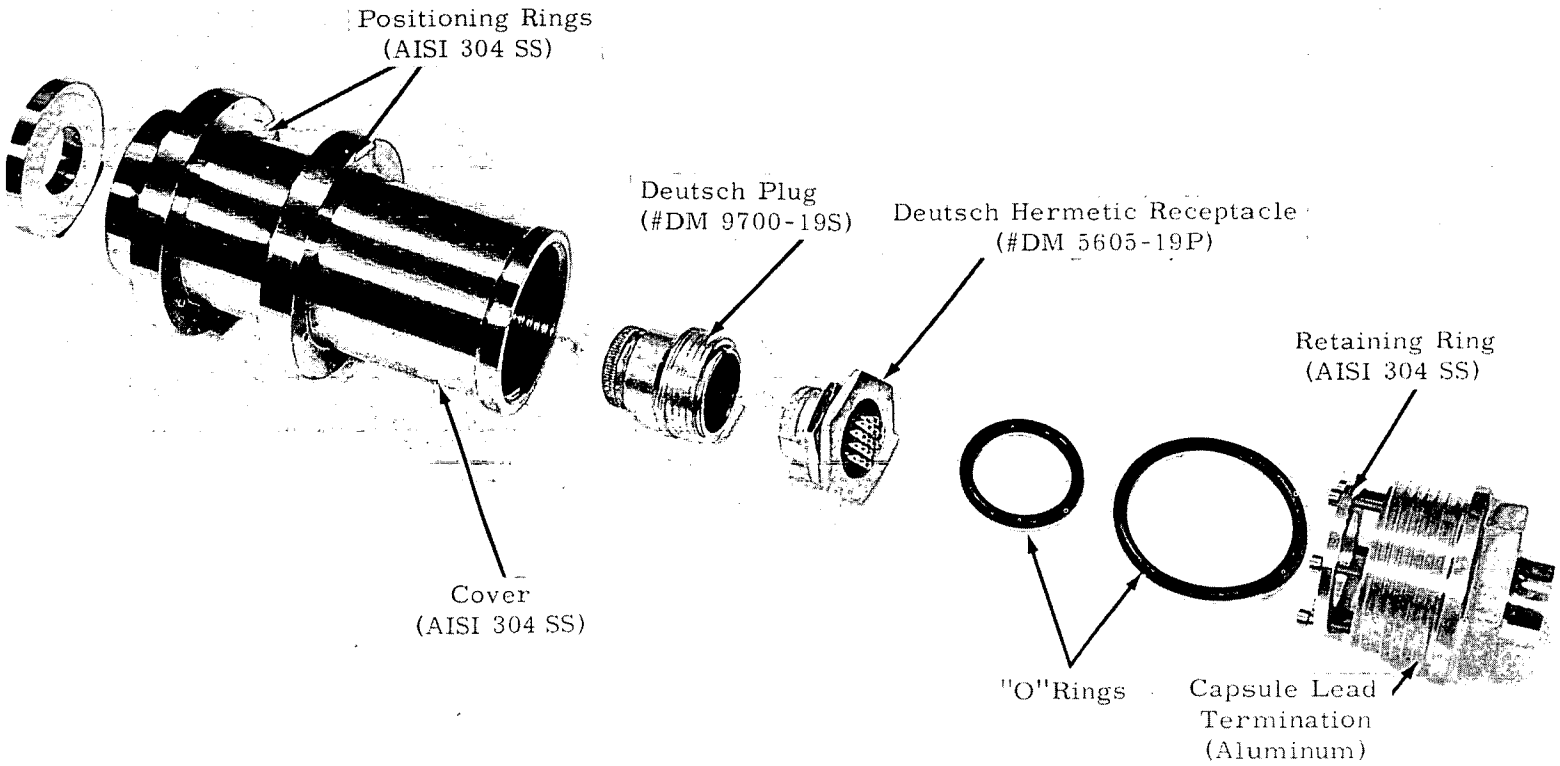

FIGURE 5

Exploded View
Capsule Primary Seal

EXPERIMENTAL PROCEDURE

Installation

The H-3-1 capsule was installed in the E-7 position of the GETR in May of 1960. Plan and elevation views of the installation are shown in Figure 6. The capsule was centered in a 2-inch diameter, Schedule-40 aluminum-pipe guide tube which had square aluminum sections welded to the ends for additional strength. The square section of the lower end was machined to the dimensions of an in-core filler piece. The upper end was attached to the loop support bracket located inside the reactor pressure vessel and immediately below the top flange. A cap which engaged the upper ring of the seal cover was attached to the guide tube to secure the capsule. Flexible steel tubing containing thermocouples connected the assembly to an access flange through a funnel tube. The lead was pressurized during irradiation.

Installation was repeated in November of 1960 with the H-3-2 experiment.

Irradiation

Initially, all nine thermocouples were operable in both capsules. H-3-1 thermocouple Number 7, located in the bottom set of samples, failed after approximately 700 hours of irradiation. The remaining eight thermocouples operated satisfactorily for the entire irradiation period of approximately 2000 hours. H-3-2 thermocouple Number 2 failed after 1750 hours, but the other eight thermocouples operated satisfactorily for the entire period. The sample temperatures reported in the section on results are mean temperatures determined from the thermocouple readings.

After 81.1 effective days of full reactor power, the H-3-1 capsule was removed from the reactor in October of 1960 and transported to the Radioactive Materials Laboratory at Vallecitos Atomic Laboratory for disassembly. The H-3-2 capsule was removed in June of 1961 after 110.6 effective days of reactor operation.

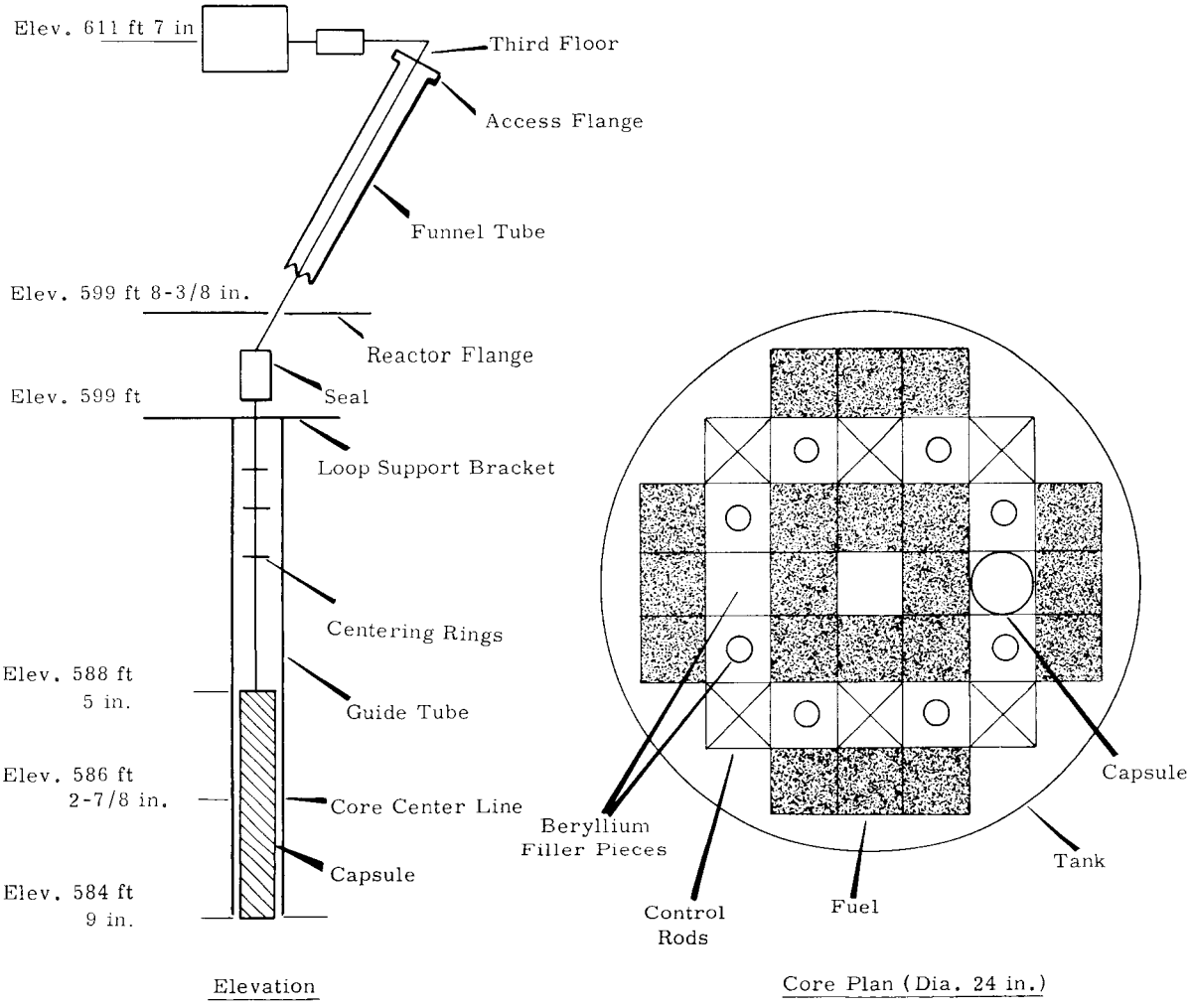

FIGURE 6

Diagram of Experiment Installation

AEC-GE RICHLAND, WASH.

Disassembly

The disassembly procedure consisted of opening the ends of the shell with a tubing cutter and then slitting the shell longitudinally with a high speed air-driven abrasive wheel. Two slits 180 degrees apart were made. The appearances of the interior of the capsules immediately after opening are shown in Figures 7 and 8. The interior surfaces were relatively clean except for some carbon deposits at the lower end. Some spacer tubes were warped. Thermocouple Number 7 in H-3-1 was bent sharply and one wire was broken. The break apparently caused the failure of the thermocouple during the irradiation. No visible changes could be related to the failure of thermocouple Number 2 in H-3-2.

The structure supporting the samples was disassembled and the samples were removed. They were all in excellent condition, with no apparent erosion. Thirty-two of the 35 flux monitors were recovered from H-3-1 and all flux monitors were recovered from H-3-2.

Postirradiation Measurements

Lengths of the irradiated samples were measured both physically and optically (see section on Sample Preparation). Results reported herein are based on the physical end-to-end measurements. The X-ray parameters, c and L_c, were measured.

Thermocouple Calibration

H-3-1 thermocouples, Numbers 2 and 5, and H-3-2 thermocouples, Numbers 3, 5, and 7, were calibrated after irradiation to check their accuracy. A new thermocouple of the same materials was used as a reference at several temperatures. The results of the calibrations are shown in Table II.

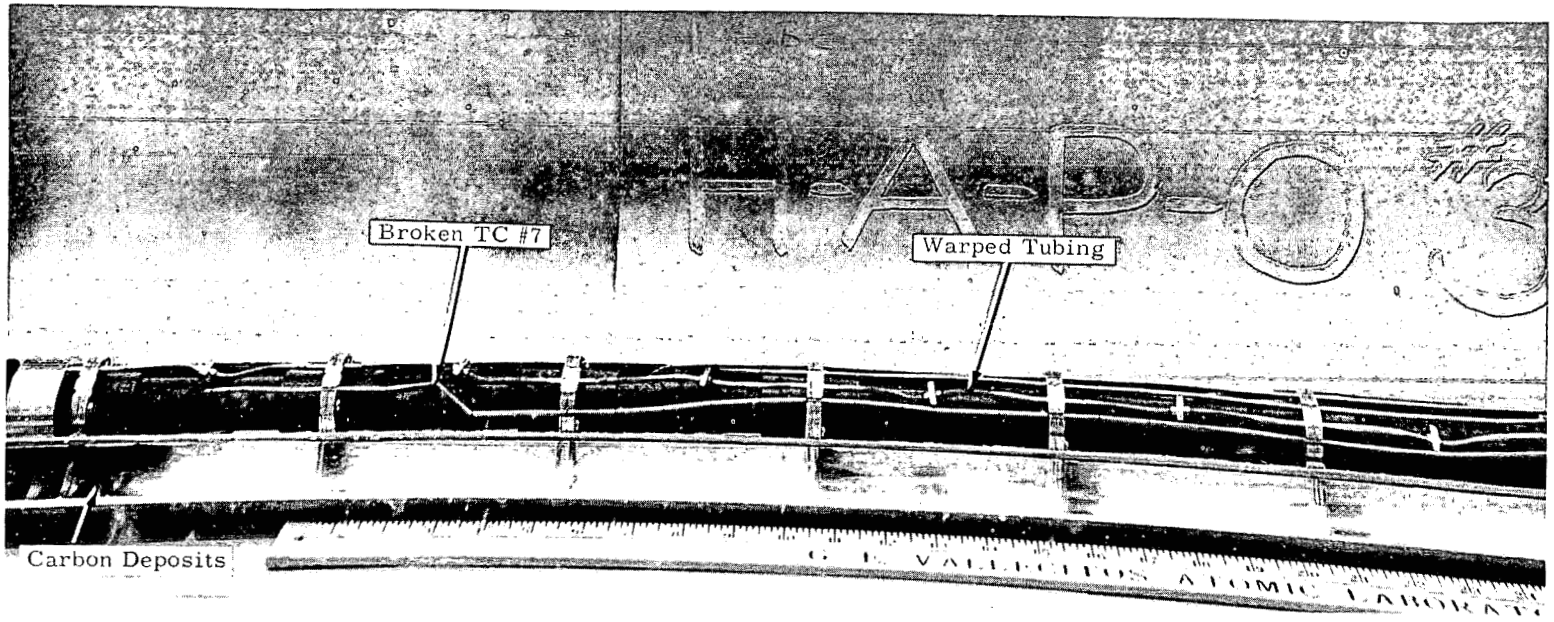

FIGURE 7

Postirradiation View of H-3-1
Curvature in Photograph is Caused by Refraction
of Lead Glass Viewing Window

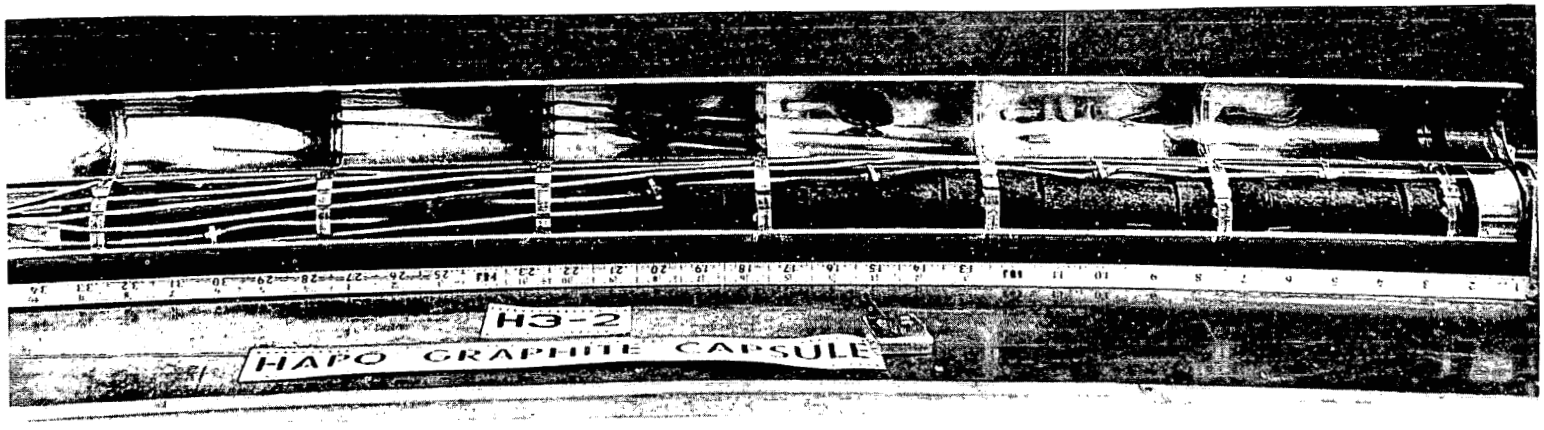

FIGURE 8

Postirradiation View of H-3-2
Curvature in Photograph is Caused by Refraction
of Lead Glass Viewing Window

TABLE II

CALIBRATION OF IRRADIATED GEMINOL N-P THERMOCOUPLES

Thermocouple	Exposure at Junction nvt x 10^{-21}, E > 0.18 Mev	Temperature, C	
Reference Thermocouple	0.0	772	377
#2	1.5	763	377
#5	2.4	760	377
Reference Thermocouple	0.0	898	508
#3	2.8	883	505
#5	3.3	869	505
#7	3.3	865	505

EXPOSURE DETERMINATION

The neutron exposure of the experiment was determined both theoretically and experimentally. The exposure to high energy neutrons was of principal interest, but thermal and resonance fluxes were also determined in order to provide a complete description of the irradiation conditions.

The PDQ code[3] was used to compute the flux in three energy groups at 5884 mesh points in one half the reactor core area. The calculation for each mesh point gave the neutron flux at the vertical point of average intensity. Furthermore, since the capsule cross sectional area included more than one mesh point, the average flux in the capsule cross section was computed.

The results of the PDQ calculation for the reactor cycles of irradiation are shown in Table III.

To determine the vertical distribution of fast flux, which is necessary for computation of the exposure of each sample in the length of the capsule, flux distributions were experimentally obtained from foils of nickel, iron, and titanium. The results of the iron and titanium foils were used only to obtain relative fluxes because their reaction cross sections are

TABLE III

E-7 FACILITY AVERAGE FLUX DURING H-3 IRRADIATIONS,

$\varphi \times 10^{-14}$

Cycle	φ_1 (> 0.18 Mev)	φ_2 (0.17 ev to 0.18 Mev)	φ_3 (< 0.17 ev)
Experiment H-3-1			
13	2.39	2.30	1.43
14 (a)	2.39	2.30	1.43
15 (b)	2.35	2.26	1.41
16	2.35	2.26	1.41
Average	2.37	2.28	1.42
Experiment H-3-2			
18	2.61	2.48	1.58
19 (c)	--	--	--
20	2.47	2.36	1.46
21	2.44	2.33	1.48
22 (d)	2.44	2.33	1.48
23	2.28	2.18	1.40
Average	2.44	2.33	1.46

(a) Not calculated: Same as Cycle 13
(b) Not calculated: Same as Cycle 16
(c) Nonoperating cycle
(d) Not calculated: Same as Cycle 21

not accurately known at this time. While nickel foils have been used extensively for fast flux monitoring, systematic burnout of the reaction products by thermal neutrons has presented problems. The current values[4] for the (n, p) products are 1650 barns for Co^{58} ($T_{1/2}$ = 71 days) and 170,000 barns for Co^{58m} ($T_{1/2}$ = 9 hours). An apparent cross section of 3750 barns was determined by the authors for correction of GETR data independent of consideration of the branching schemes and cross sections of the nickel reaction.[5]

The methods of analyzing the foils from the H-3-1 experiment and the results obtained were used in determining the longitudinal distribution described in Appendix B. With the knowledge of the longitudinal variation and the calculated average flux, the exposures for all samples were determined and the results are shown in Table IV.

TABLE IV

VARIATION OF EXPOSURE AS A FUNCTION OF SAMPLE POSITION

		Fast				Thermal			
			nvt x 10^{-21}, E > 0.18 Mev				nvt x 10^{-21}, E < 0.17 ev		
Position	Core Elevation	Mean Ratio	H-3-1	H-3-2	Total	Mean Ratio	H-3-1	H-3-2	Total
PDQ Average		1.00	1.66	2.33		1.00	1.00	1.40	
1	31.1	0.55	0.92	1.29	2.21	0.47	0.47	0.66	1.13
2	25.9	0.91	1.51	2.12	3.63	0.95	0.95	1.33	2.28
3	20.8	1.22	2.03	2.84	4.87	1.20	1.20	1.68	2.88
4	15.6	1.43	2.37	3.33	5.70	1.41	1.41	1.97	3.38
5	10.6	1.42	2.36	3.31	5.67	1.40	1.40	1.96	3.36
6	5.4	1.04	1.73	2.42	4.15	1.06	1.06	1.48	2.54
Core Bottom	0								

EXPOSURE EQUIVALENCE

Almost all exposure data on radiation to graphite have been reported in megawatt days per adjacent ton of uranium (MWD/AT) or some related parameter. The term MWD/AT is not an expression of exposure which is universally related to damage if the neutron spectra of the reactors compared are not identical. Such factors as geometry, moderator-to-uranium ratio, and degree of enrichment affect the neutron spectrum. Therefore, it is preferred to express data in terms of the primary exposure units known for the irradiation conditions. Adjustment to other units can be made later based on the best estimate of equivalence. In this report, exposure to neutrons whose energy is in excess of 0.18 Mev is used. Many calculations of EGCR exposure rates have been performed in both nvt and MWD/AT. The value 1 MWD/AT = 1.5×10^{17} nvt(E>0.18 Mev) was developed based on a comparison of damaging flux of the EGCR and GETR spectra relative to neutrons of E>0.18 Mev.[6]

The spectrum of the testing position used for the irradiation is shown in Figure 9. This spectrum was calculated by Preskitt using the GNU-II code modified to include 20 groups above 0.18 Mev.[7] GNU-II is a radial code and some inaccuracies result from the homogenizing of the radius increment at the E-7 position. The dip in the spectrum is caused by beryllium in that increment.

IRRADIATION RESULTS

The two capsule experiments performed in the GETR extend the knowledge of physical distortion effects induced by neutron irradiation to an equivalent of 38,000 MWD/AT (EGCR). The exposure achieved is the highest of any graphite irradiation experiment reported. Auxiliary to the study of physical distortion, X-ray measurements were made to evaluate crystallite damage, using the parameters $\underline{c}$ and L_c.

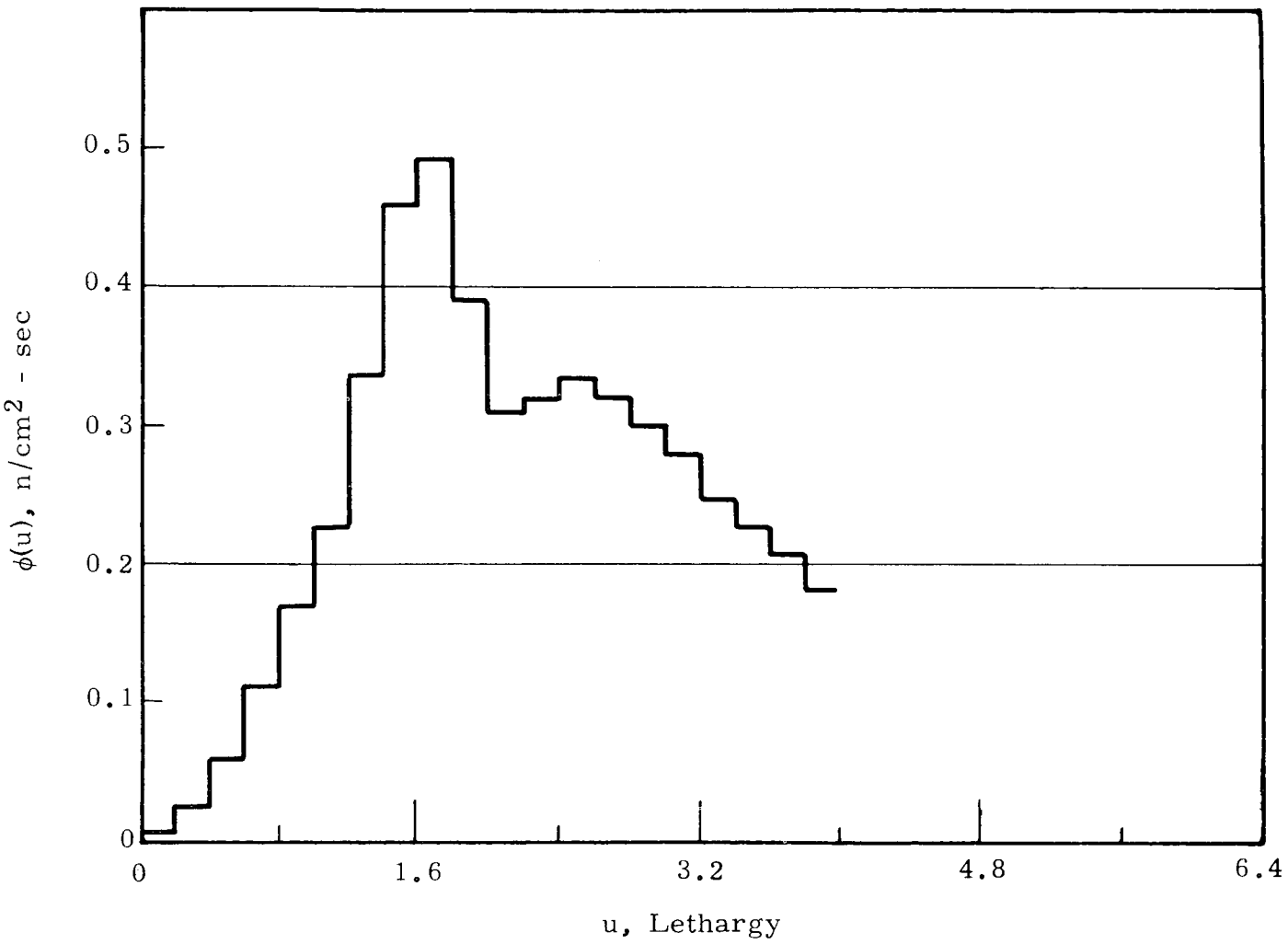

FIGURE 9

Neutron Spectral Distribution in E-7
The Intergral Between Lethargy 0 and 4 Has Been Normalized
to One Neutron Per cm^2 Per Second

Complete results of the H-3-1 and H-3-2 capsules are given in Tables V and VI. The asterisk adjacent to the sample type in Table VI indicates a new sample at that position for the H-3-2 irradiation. The notations (1), (2), and (3) refer to the positions from which parallel samples were taken: the edge, the midpoint, and the center of the bar.

High Temperature Contraction

The distortion data in Tables V and VI have been expressed graphically in Figures 10 through 13. The isotherms of the effect of exposure on distortion indicate a lessening of contraction rate at temperatures in the vicinity of 800 C. These data supplement the information on temperature sensitivity of high temperature irradiation previously reported by the authors.[8]

Graphite of the EGCR type undergoes initial expansion at low exposures during high temperature irradiations.[9] The expansion, while not thoroughly understood, usually reaches a maximum at 0.01 to 0.02 per cent at an exposure of 0.25×10^{21} nvt, and is greater in the transverse than in the parallel direction. This expansion is not the relief of strain induced during preparation of the sample. Strain induced during sample preparation can be relieved by thermal annealing at high temperatures after the samples are made; samples used in the H-3 experiments were annealed at 1900 C. The curves presented here show the estimated growth during early irradiation; taking this growth into consideration permits a reasonable, nearly linear connection of data from the H-3-1 and H-3-2 experiments.*

---

* Recipients of preliminary results of the H-3-1 experiment will recall that the distortion rates then were computed on the basis of a linear connection to the origin. With only zero and terminal points of contraction known, serious deflection in slope could occur with small errors in selection of maximum growth and exposure at maximum growth. With data from two exposures available now, initial growth should be considered in the correlation of the data.

TABLE V

H-3-1 EXPERIMENTAL RESULTS

Temperature, C	Exposure, nvt × 10^{-21} (E > 0.18 Mev)	Sample Code	Length Changes, Per Cent ΔL/L	X-Ray Changes, Å: c Initial	c Δc	L_c Initial	L_c ΔL_c
450 ± 25	0.92	CSF⊥	-0.058 ± 0.001	6.718	+0.014	700	-380
		NC7⊥	-0.040 ± 0.001	6.722	+0.013	645	-325
		CSF∥	-0.105 ± 0.002	6.722	+0.011	720	-415
		NC7∥ (1)	-0.112 ± 0.001	6.732	0	610	-300
575 ± 25	1.51	CSF⊥	-0.067 ± 0.002	6.718	+0.010	685	-210
		NC7∥ (1)	-0.114 ± 0.001	6.715	+0.010	685	-320
		NC7∥ (2)	-0.123 ± 0.002	6.717	+0.015	720	-300
		NC7∥ (3)	-0.124 ± 0.001	6.702	+0.028	440	- 85
725 ± 25	2.03	CSF⊥	-0.044 ± 0.002	6.707	+0.014	600	-275
		NC7⊥	-0.021 ± 0.001	6.717	+0.005	700	-370
		CSF∥	-0.099 ± 0.001	6.720	+0.006	680	-360
		NC7∥ (1)	-0.113 ± 0.001	6.717	+0.002	675	-360
825 ± 25	2.37	CSF⊥	-0.054 ± 0.002	6.724	-0.006	600	-285
		NC7∥ (1)	-0.159 ± 0.001	6.736	-0.015	650	-347
		NC7∥ (2)	-0.140 ± 0.002	6.736	-0.011	620	-340
		NC7∥ (3)	-0.146 ± 0.002	6.756	-0.034	600	-297
850 ± 25	2.36	CSF⊥	-0.064 ± 0.001	6.739	-0.021	630	-315
		NC7⊥	-0.042 ± 0.002	6.722	+0.001	645	-255
		CSF∥	-0.164 ± 0.002	6.734	-0.023	580	-331
		NC7∥ (1)	-0.166 ± 0.001	6.732	-0.014	720	-410
625 ± 25	1.73	CSF⊥	-0.067 ± 0.002	6.722	+0.008	595	-235
		NC7⊥	-0.041 ± 0.002	6.736	-0.008	700	-235
		CSF∥	-0.108 ± 0.002	6.722	+0.003	685	-350
		NC7∥(1)	-0.095 ± 0.002	6.736	-0.006	635	-185

TABLE VI

H-3-2 EXPERIMENTAL RESULTS

Temperature, C	Exposure, nvt $\times 10^{-21}$ (E > 0.18 Mev)	Sample Code	Length Changes, Per Cent $\Delta L/L$	X-Ray Changes, Å			
				c		L_c	
				Initial	Δc	Initial	ΔL_c
475 ± 25	2.21	CSF⊥	-0.223 ± 0.001	6.718	+0.040	700	-501
	2.21	NC7⊥	-0.186 ± 0.001	6.722	+0.038	645	-405
	1.29	*CSF∥	-0.143 ± 0.002	6.720	+0.028	570	-310
	2.21	NC7∥ (1)	-0.363 ± 0.002	6.732	+0.023	610	-380
575 ± 25	3.63	CSF⊥	-0.283 ± 0.002	6.718	+0.021	685	-465
	3.63	NC7∥ (1)	-0.438 ± 0.001	6.715	+0.037	685	-435
	2.12	*NC8∥ (2)	-0.203 ± 0.002	6.719	+0.023	595	-315
	2.12	*NC8∥ (3)	-0.212 ± 0.002	6.707	+0.031	485	-202
725 ± 25	2.84	*CSF⊥	-0.120 ± 0.002	6.725	+0.013	560	-290
	2.84	*NC8⊥	-0.144 ± 0.001	6.722	+0.010	762	-483
	2.84	*CSF∥	-0.228 ± 0.001	6.730	+0.008	420	-172
	2.84	*NC8∥ (1)	-0.231 ± 0.002	6.725	+0.015	680	-437
800 ± 25	3.33	*CSF⊥	-0.114 ± 0.002	6.731	-0.003	560	-299
	3.33	*NC8∥ (1)	-0.227 ± 0.002	6.723	+0.005	735	-492
	5.70	NC7∥ (2)	-0.662 ± 0.001	6.736	-0.004	620	-407
	5.70	NC7∥ (3)	-0.634 ± 0.002	6.756	-0.023	600	-411
775 ± 25	5.67	CSF⊥	-0.324 ± 0.001	6.739	-0.007	630	-411
	5.67	NC7⊥	-0.222 ± 0.002	6.722	+0.016	645	-421
	5.67	CSF∥	-0.643 ± 0.002	6.734	+0.001	580	-363
	5.67	NC7∥ (1)	-0.653 ± 0.001	6.732	+0.004	720	-510
625 ± 25	4.15	CSF⊥	-0.253 ± 0.001	6.722	+0.002	595	-363
	4.15	NC7⊥	-0.227 ± 0.002	6.736	+0.009	700	-442
	4.15	CSF∥	-0.399 ± 0.002	6.722	+0.022	685	-393
	4.15	NC7∥ (1)	-0.397 ± 0.002	6.736	+0.006	635	-385

* New sample

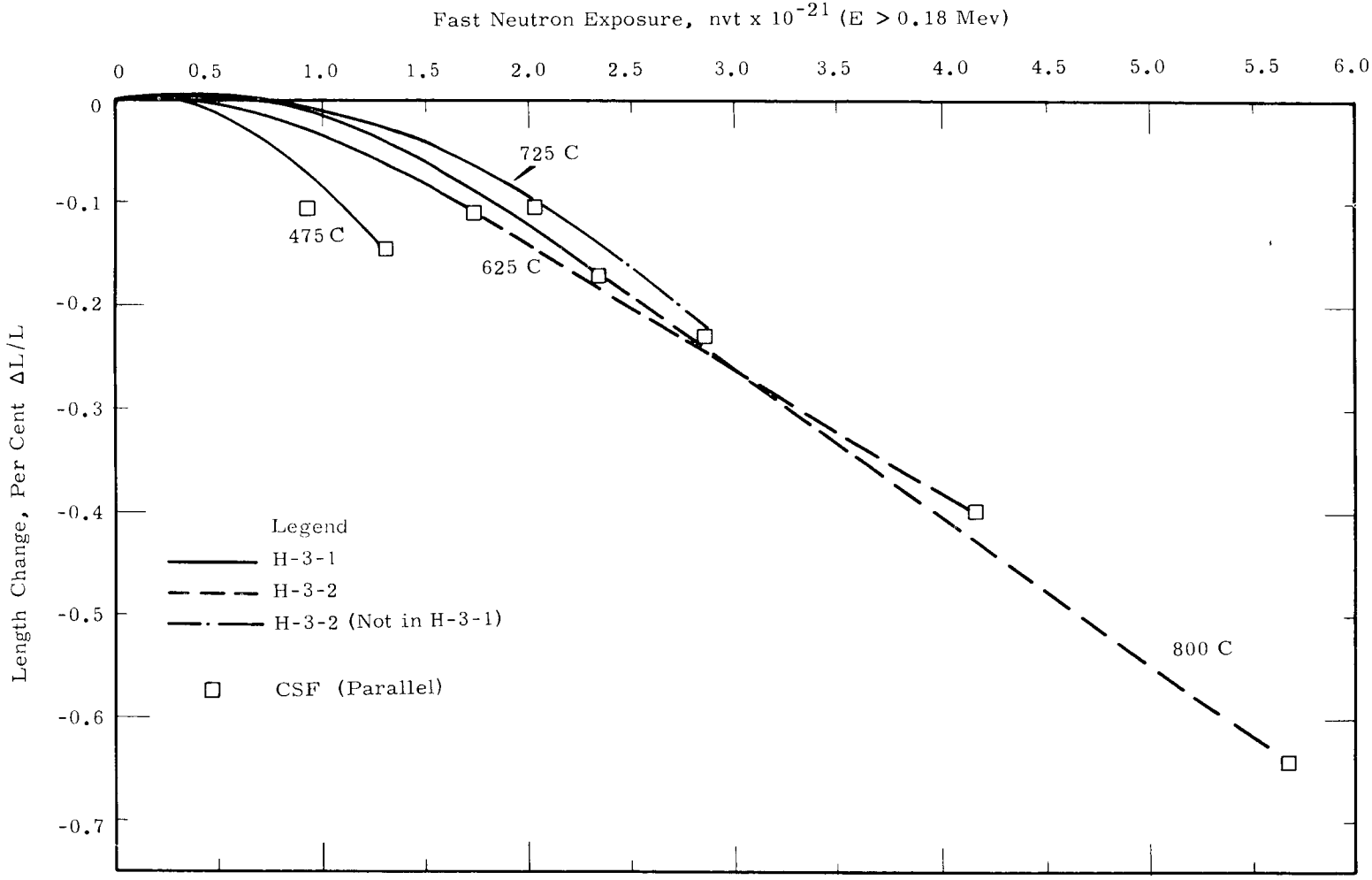

FIGURE 10

Contraction Behavior of CSF Graphite (Parallel)
as a Function of Exposure

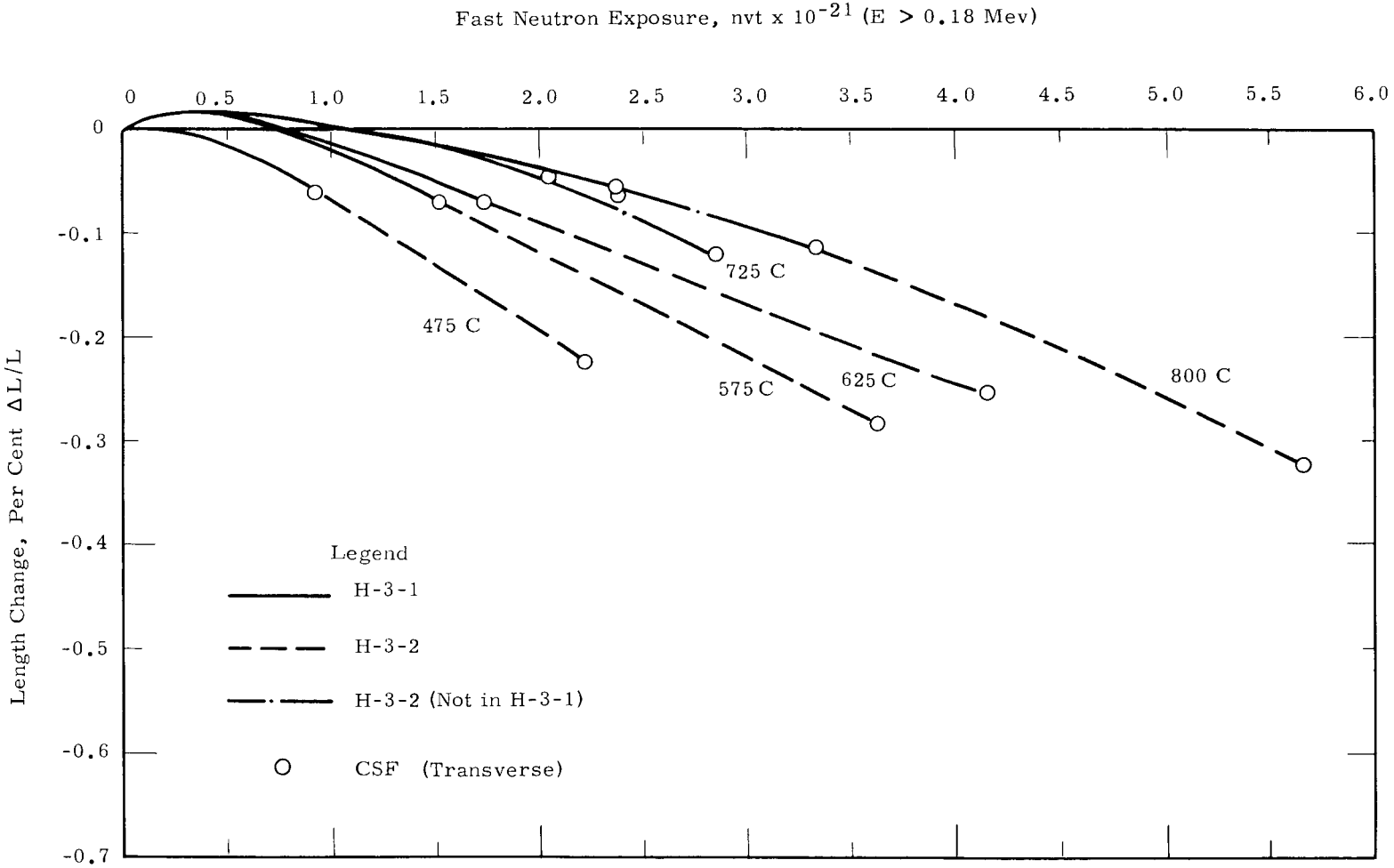

FIGURE 11

Contraction Behavior of CSF Graphite (Transverse)
as a Function of Exposure

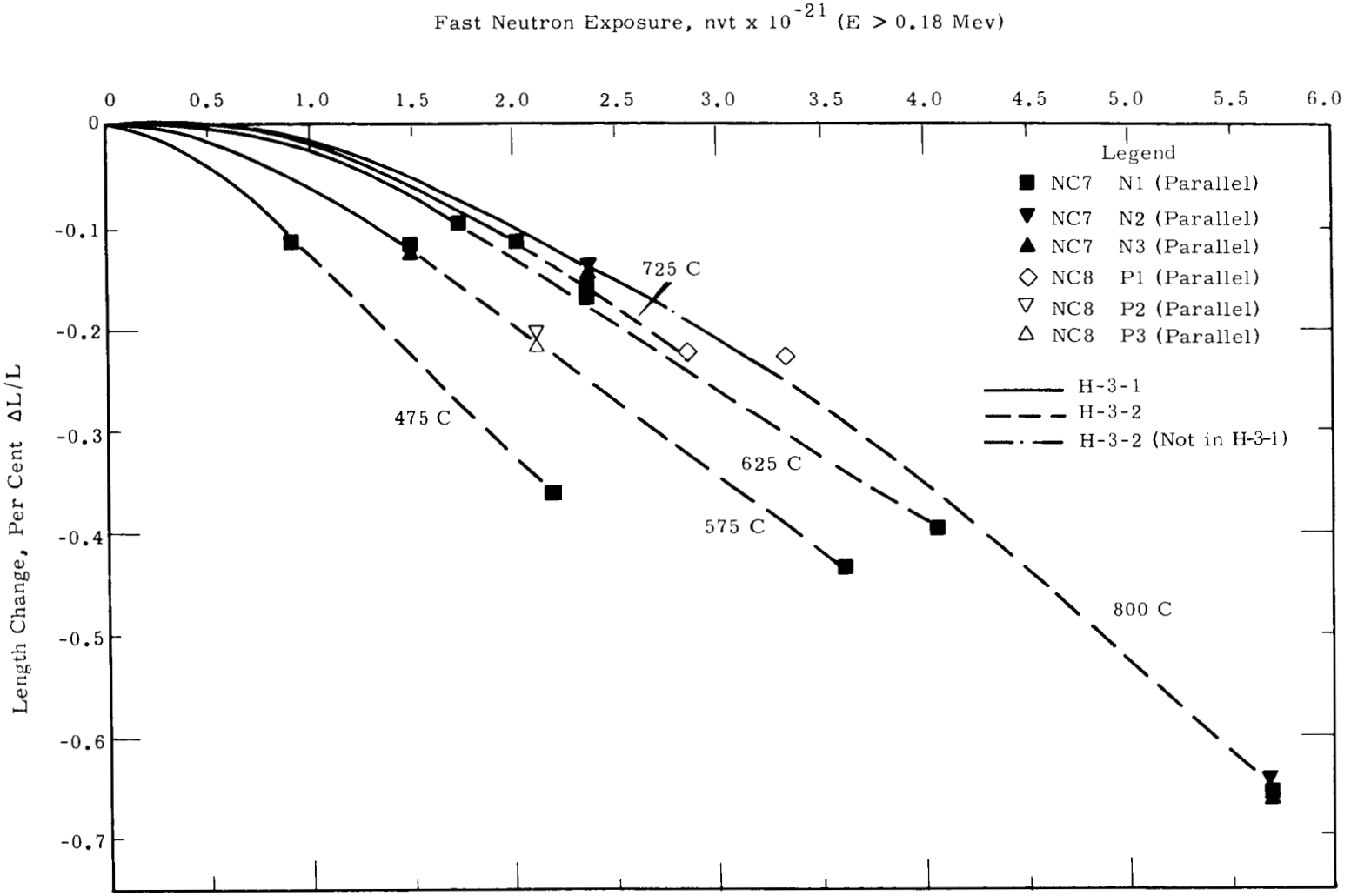

FIGURE 12

Contraction Behavior of EGCR Graphites (Parallel)
as a Function of Exposure

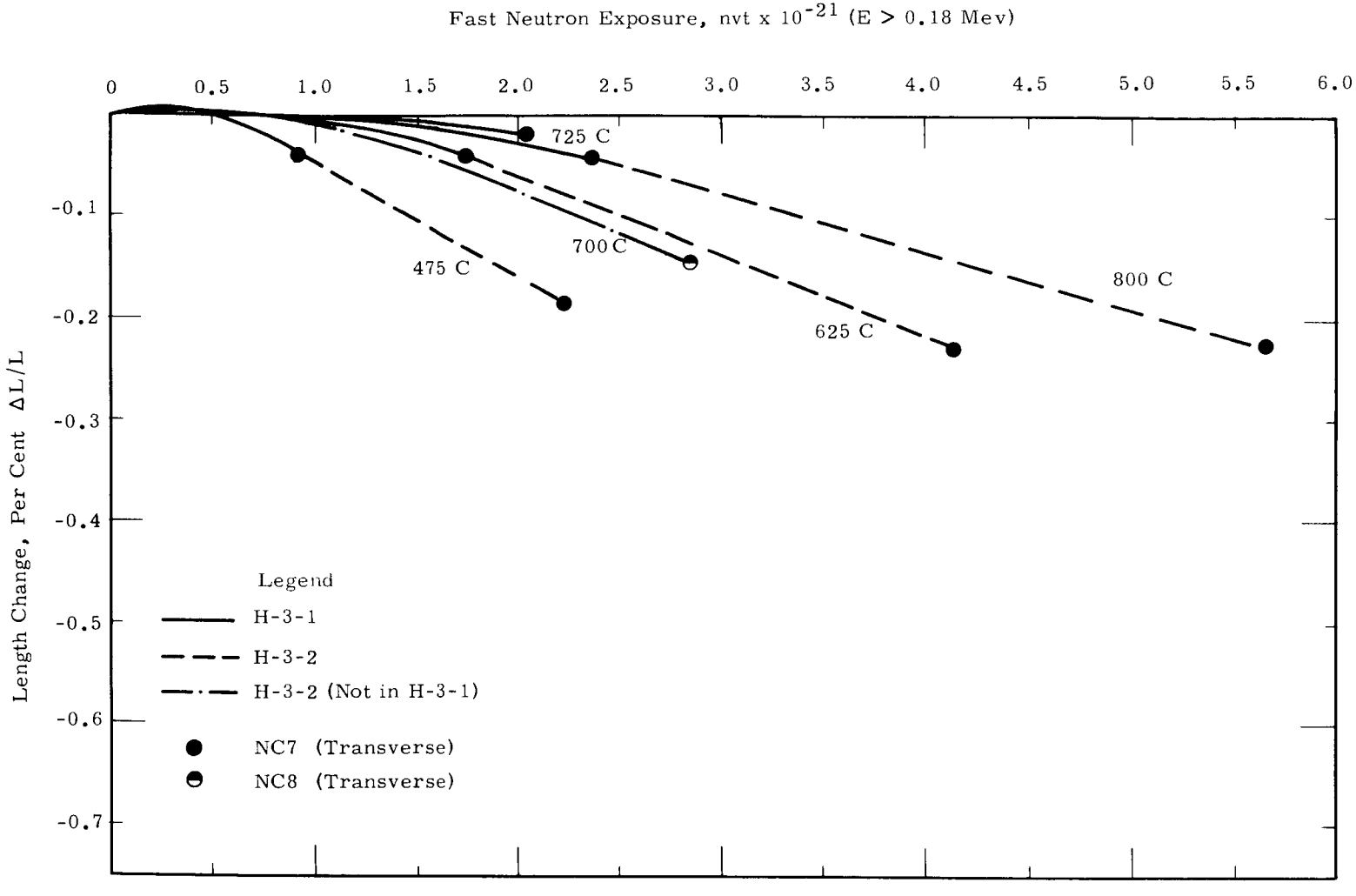

FIGURE 13

Contraction Behavior of EGCR Graphites (Transverse)
as a Function of Exposure

The EGCR prototype graphite, NC-7, appears to be approximately equivalent in damage characteristics to actual EGCR graphite, NC-8. Overlap of data occurs at similar exposures and smooth curves can be drawn from the data for both types.

At the initiation of the experiment, it was not known to what extent the particle alignment patterns caused by the extrusion die would affect contraction rates of parallel samples taken near the center, midpoint, and edge of the extrusion. Different contraction rates could seriously complicate the calculation of stress variation within EGCR moderator blocks. Fortunately, the testing of samples N-1, N-2, and N-3 from NC-7 and of samples P-1, P-2, and P-3 from NC-8 showed no significant differences in contraction behavior due to differences of sample location in the extruded bar.

There is no indication, based on data available at this time, that the rate of contraction lessens with continuing exposure.

Changes in X-ray Parameters

Figures 14 through 21 show the result of continued irradiation on crystallite dimensions $\underline{c}$ and L_c. $\underline{c}$ is defined as the distance between alternate layer planes. L_c is the apparent crystallite size in the c-direction. The data are arbitrarily presented in four figures to alleviate confusion resulting from the number of curves shown. The data for the transverse and parallel orientations should be considered together and not as independent results.

In terms of crystallite damage, all graphites tested behaved similarly. There is a marked change in $\underline{c}$ as a function of temperature and exposure, although the transition is not as continuous as L_c. The changes in $\underline{c}$ at an exposure 1 to 3 x 10^{21} may reflect a change in damage mechanism. Both the EGCR and CSF graphites seem to have stabilized at a value of L_c of approximately 200-250 Å despite differences in irradiation temperature and final exposure. The next irradiation period may indicate whether the stabilization noted is a saturation in the property change.

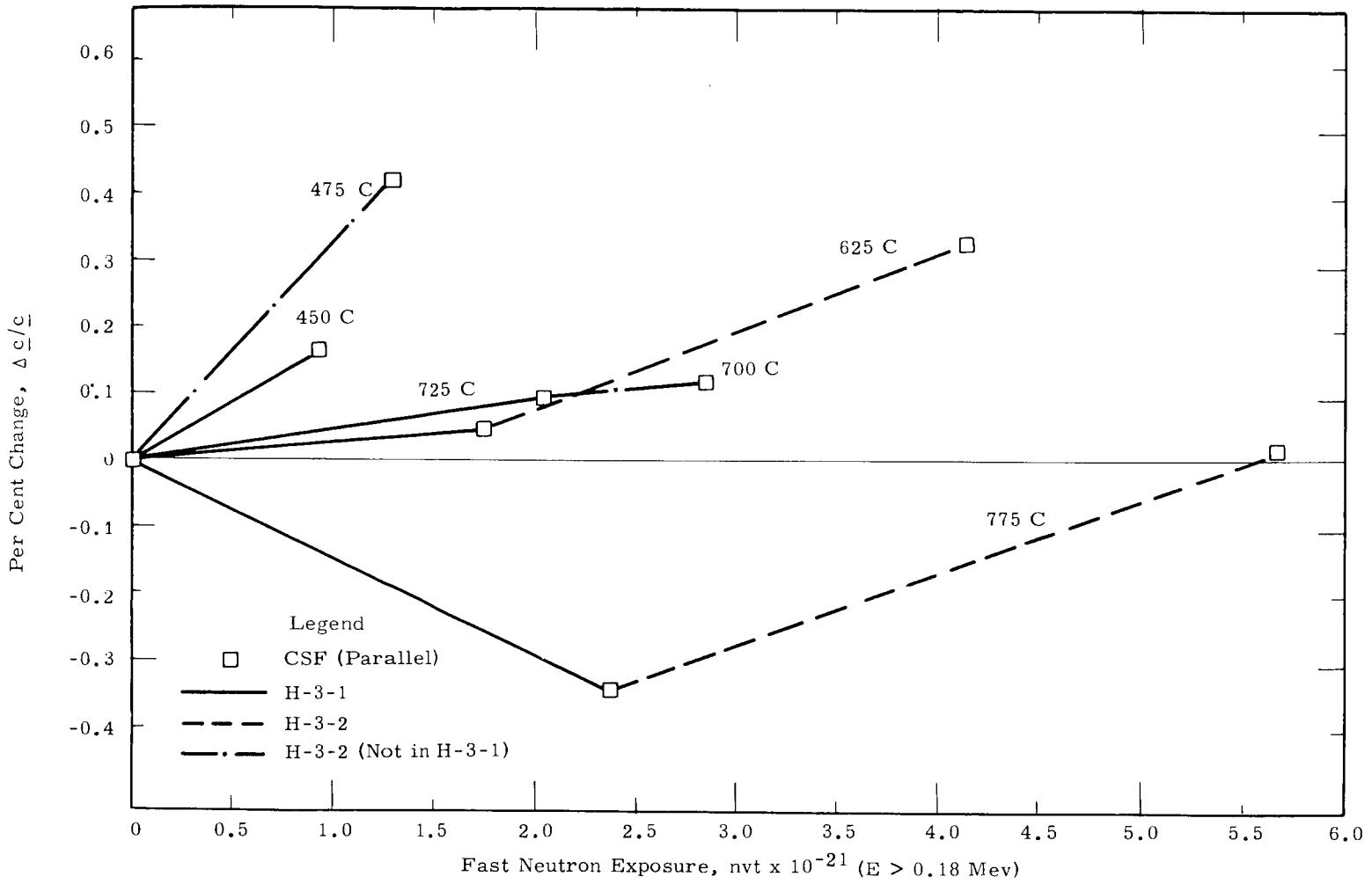

FIGURE 14

Effect of Irradiation on Layer Spacing
CSF Graphite
Indication of Extrusion Direction is for Sample Identification and Plotting Convenience.
Refer Also to Companion Graph for the Same Graphite.

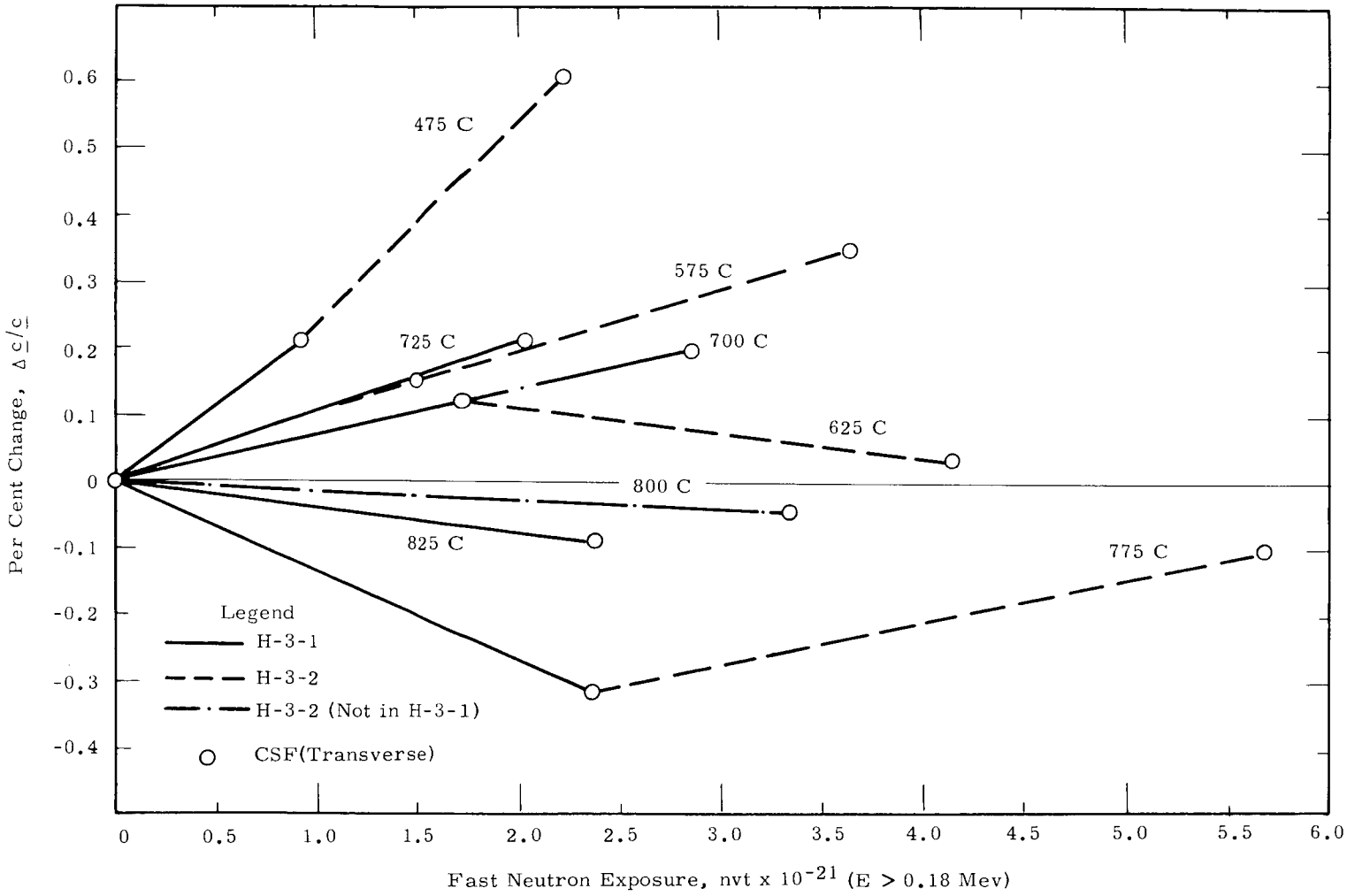

FIGURE 15

Effect of Irradiation on Layer Spacing
CSF Graphite
Indication of Extrusion Direction is for Sample Identification and Plotting Convenience.
Refer also to Companion Graph for the Same Graphite.

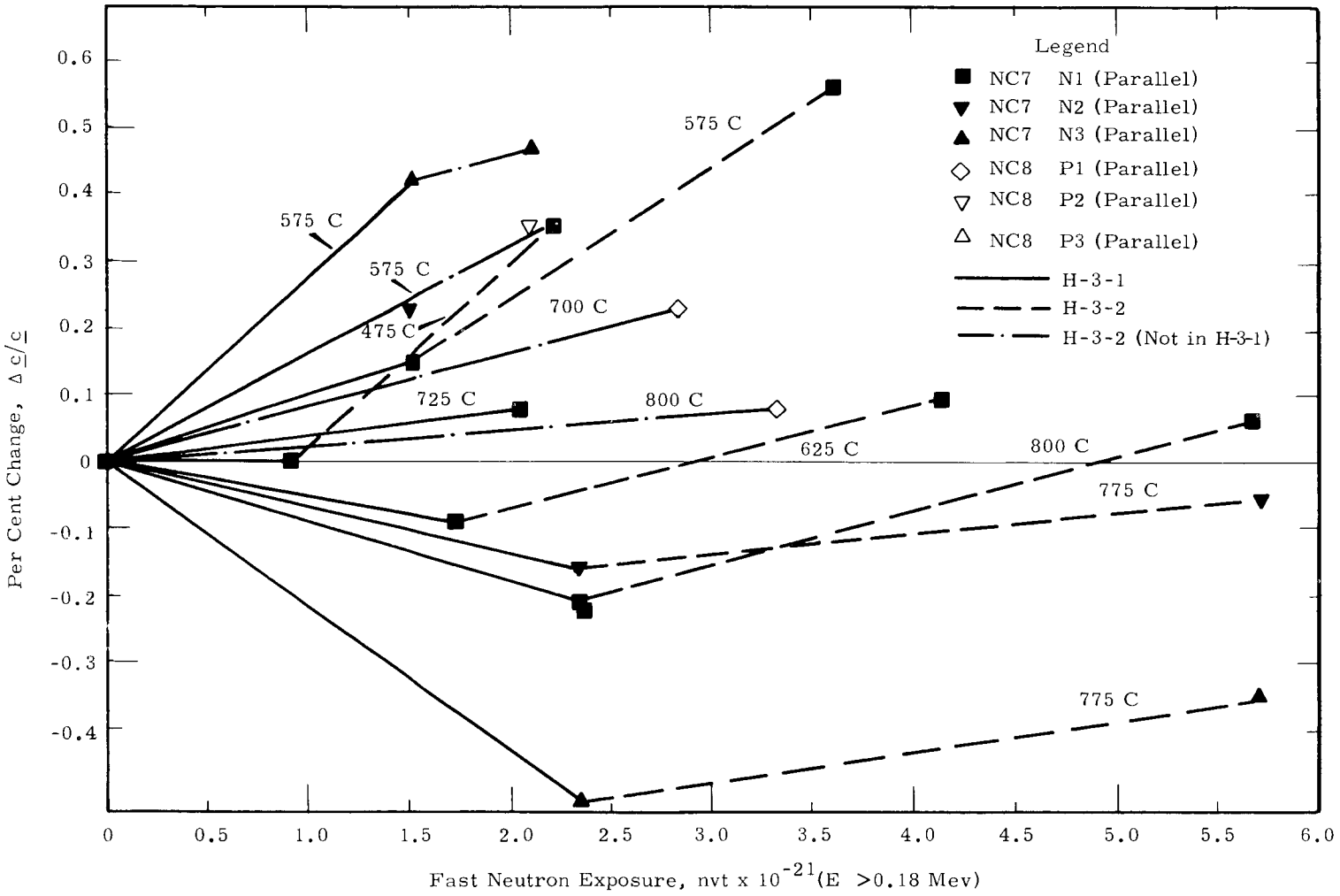

FIGURE 16

Effect of Irradiation on Layer Spacing
EGCR Graphite
Indication of Extrusion Direction is for Sample Identification and Plotting Convenience.
Refer also to Companion Graph for the Same Graphite.

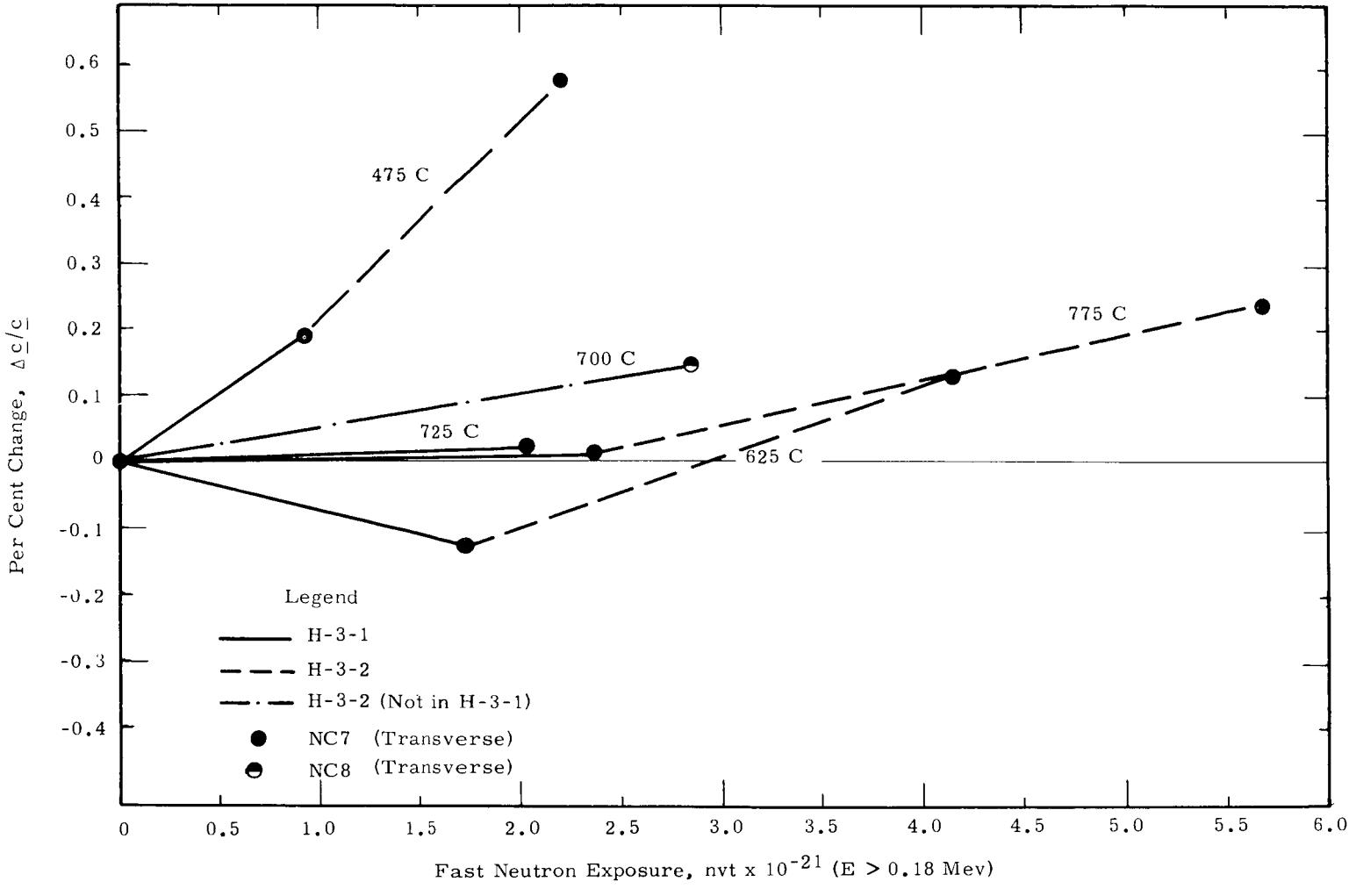

FIGURE 17

Effect of Irradiation on Layer Spacing
EGCR Graphite
Indication of Extrusion Direction is for Sample Identification and Plotting Convenience.
Refer Also to Companion Graph for the Same Graphite.

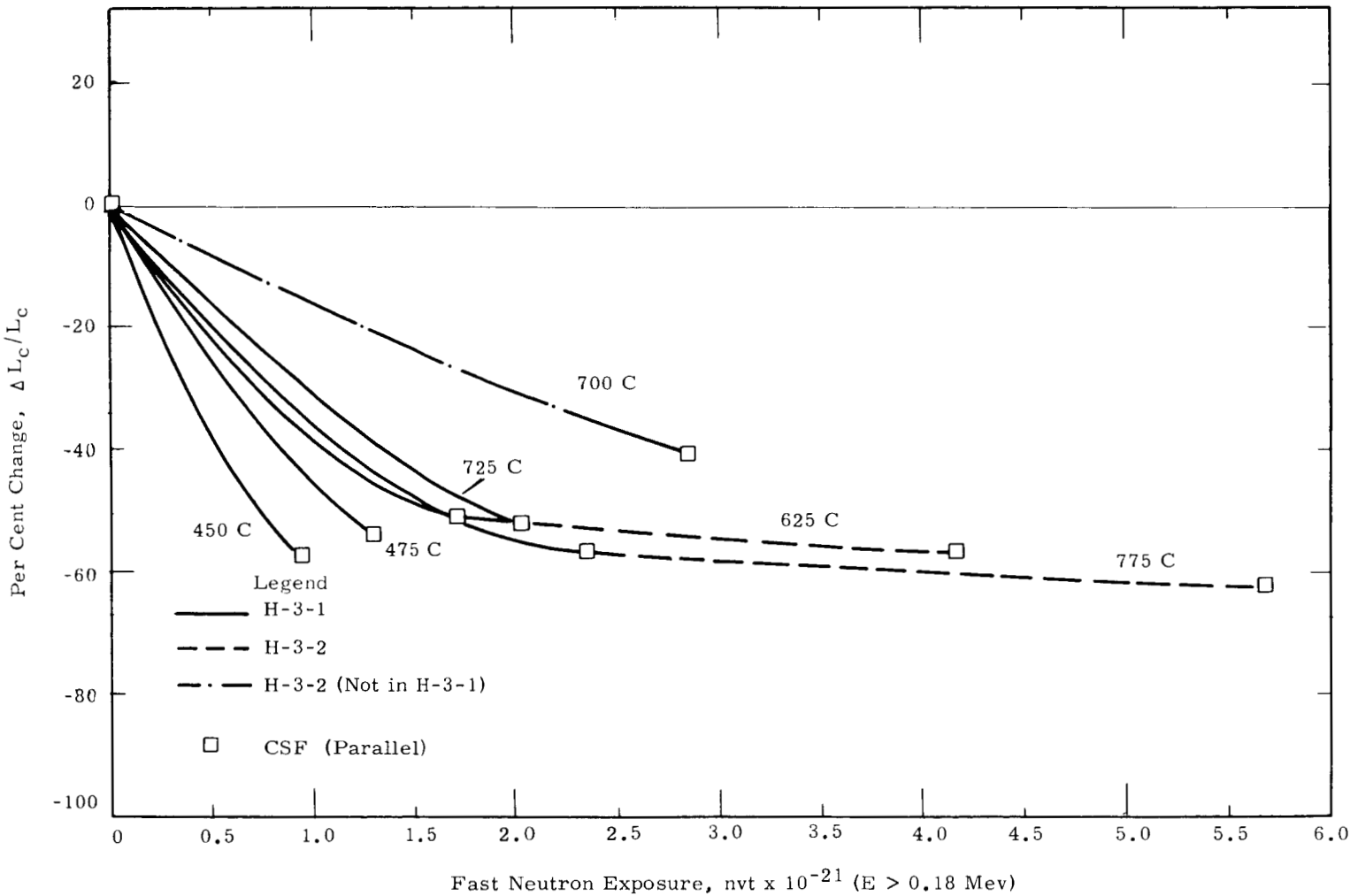

FIGURE 18

Effect of Irradiation on Apparent Crystallite Size
CSF Graphite
Indication of Extrusion Direction is for Sample Identification and Plotting Convenience.
Refer Also to Companion Graph for the Same Graphite.

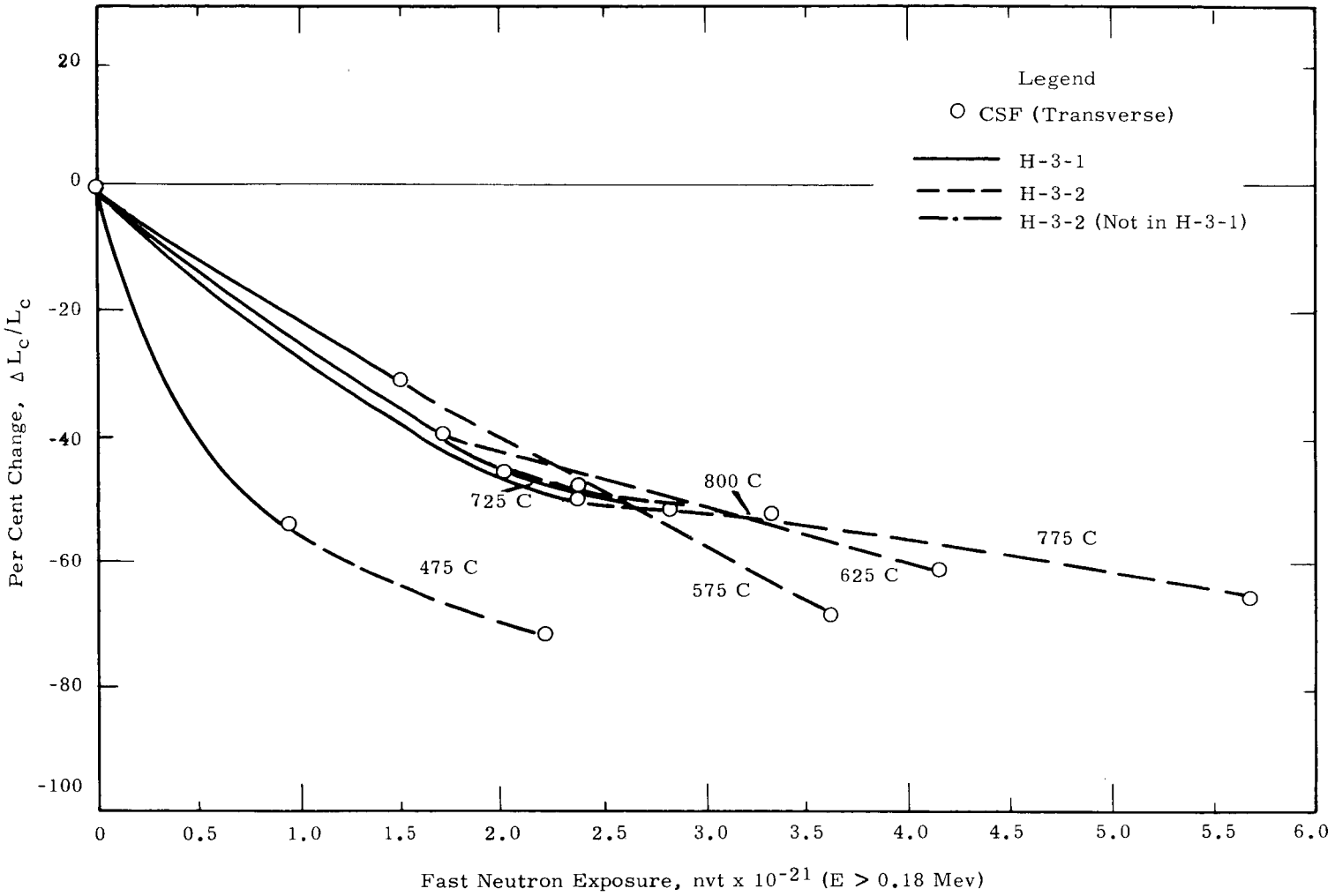

FIGURE 19

Effect of Irradiation on Apparent Crystallite Size
CSF Graphite
Indication of Extrusion Direction is for Sample Identification and Plotting Convenience.
Refer Also to Companion Graph for the Same Graphite.

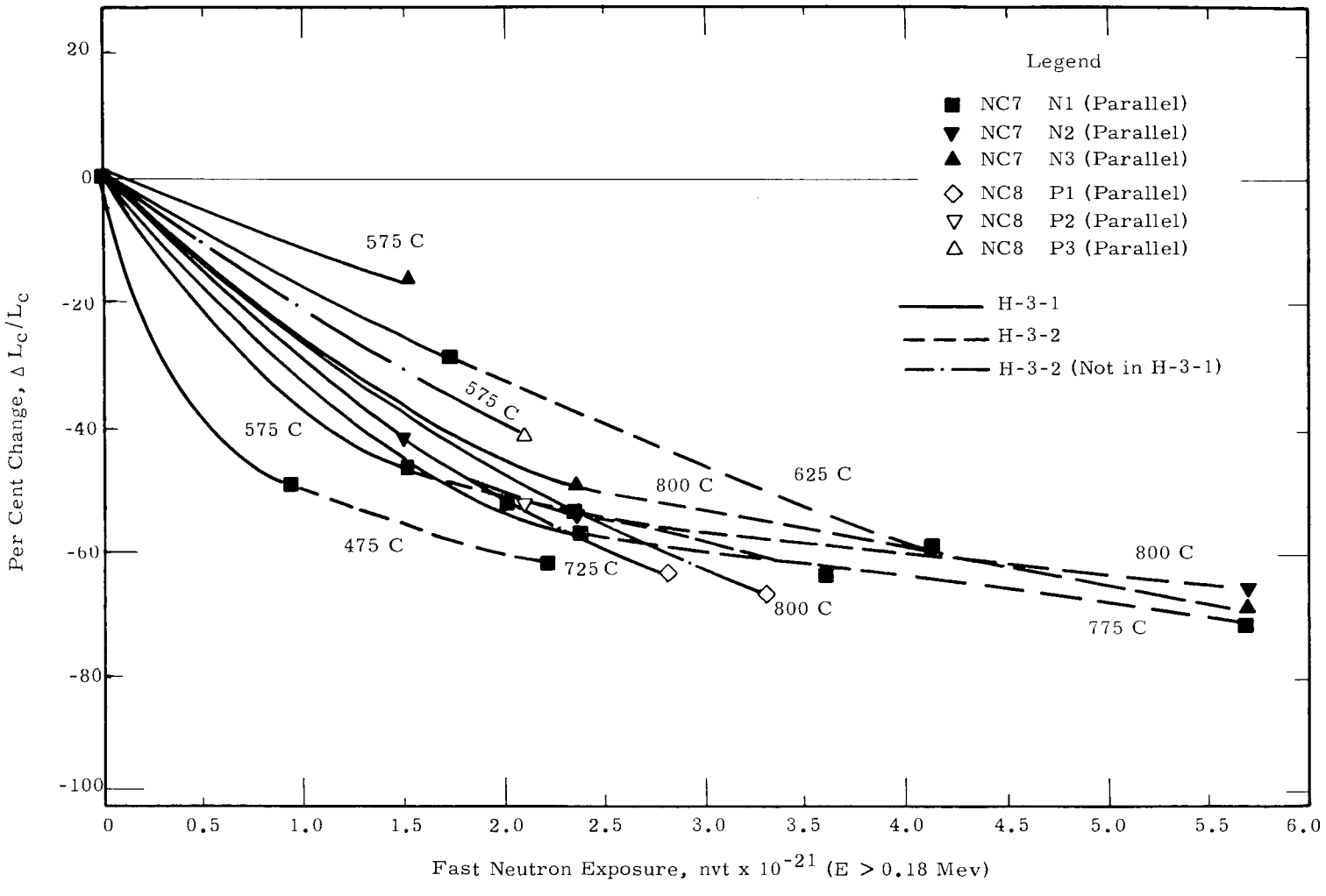

FIGURE 20

Effect of Irradiation on Apparent Crystallite Size
EGCR Graphite
Indication of Extrusion Direction is for Sample Identification and Plotting Convenience.
Refer Also to Companion Graph for the Same Graphite.

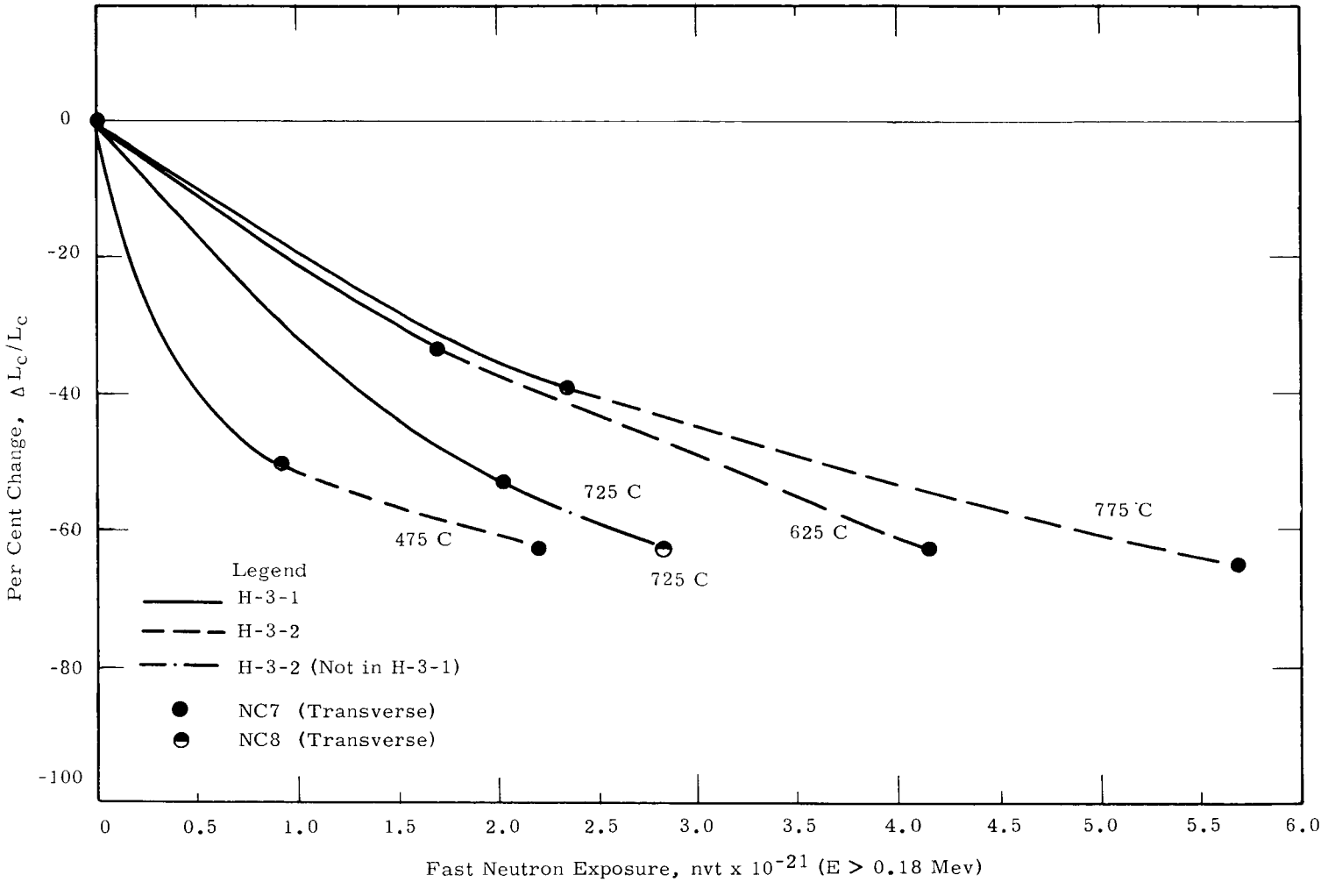

FIGURE 21

Effect of Irradiation on Apparent Crystallite Size
EGCR Graphite
Indication of Extrusion Direction is for Sample Identification and Plotting Convenience.
Refer Also to Companion Graph for the Same Graphite.

Application of Results to the EGCR

The purpose of the H-3 irradiation series is to determine the effect of neutron irradiation on EGCR graphite to exposures comparable with the design lifetime of the EGCR. Some of the specific results sought are the rate of contraction, the effect of temperature on the rate of contraction, and the extent of contraction at saturation if saturation occurs at less than full lifetime exposure.

Based on the best estimates of interreactor conversion factors, the rate of contraction of EGCR graphite is within design limits which were based on early estimates by Hanford. The rate of distortion, after initial growth, of EGCR parallel samples at the peak EGCR temperature (575 C) is -0.15 per cent per 10^{21} nvt. Based on current conversion factors, the rate expressed in terms of MWD/AT is -0.023 per cent per 1000 MWD/AT. At a lower temperature (475 C) the rate is -0.19 per cent per 10^{21} nvt or -0.028 per cent per 1000 MWD/AT. No saturation of contraction has been observed and it is believed that the data can be extrapolated somewhat. However, since no other graphite data exist for exposures higher than reported here, extrapolation should be made cautiously.

The possible effects of neutron intensity differences on high temperature contraction is being studied elsewhere.* Until data confirm the belief that the effect is small or nonexistent, the results reported here should be used with appropriate caution.

ACKNOWLEDGMENTS

The authors wish to thank C. A. Preskitt of the Oak Ridge National Laboratory for computing the neutron spectrum of the GETR which was instrumental in evaluating the irradiation data.

Capsule assembly and sample measurements were conducted largely by W. E. Hart and F. D. Hobbs.

---

* The Hanford GEH-13 experiment in the Engineering Test Reactor (ETR) is designed to show the effect, if any, of flux intensity at high irradiation temperatures.

NOTES ADDED IN PRESS

Preliminary results of the H-3-3 experiment, which extend the peak exposure to 8.7×10^{21} nvt, confirm and extend the results reported in this document. Based on these preliminary data, the contraction rate of transverse samples continues linearly to the foregoing exposure. Parallel samples show a slight acceleration of contraction. The temperature coefficient of contraction still is present, but is greater for the transverse samples. Unexpectedly, NC-7 seems to be diverging from NC-8.

The H-3-4 capsule is now undergoing irradiation in the GETR. The next interim report (HW-71500 B) will present data from the H-3-3 and H-3-4 capsules.

REFERENCES

1. Davidson, J. M. Thermally Induced Length Changes of Graphite Cubes, HW-65815. June 24, 1960.
2. Davidson, J. M. and J. W. Helm. The H-1 High Temperature Graphite Irradiation Experiment, HW-64286. April, 1961.
3. Bilodeau, G. G., et al. PDQ - An IBM-704 Code to Solve the Two-Dimensional Few-Group Neutron-Diffusion Equations, WAPD-TM-70. August, 1957.
4. Hogg, C. H., et al. "Thermal Neutron Cross Sections of Co^{58} Isomers and the Effect on Fast Flux Measurements Using Nickel," Trans. Am. Nuclear Soc., 4, No. 2: 271. November, 1961.
5. Davidson, J. M. and J. W. Helm. op cit., HW-64286, page 41.
6. de Halas, D. R. Personal Communications. October, 1960.
7. Preskitt, C. A. Personal Communications. June, 1960.
8. Davidson, J. M. and J. W. Helm. "Effect of Temperature on Radiation-Induced Contraction of Reactor Graphite," Proceedings of the Fifth Carbon Conference, Pennsylvania State University, 1962. To be published.
9. Davidson, J. M., et al. "High Temperature Radiation Induced Contraction in Graphite," Proceedings of the Fourth Carbon Conference, Buffalo: 599-605. 1960.
10. McAdams, W. H. Heat Transmission, 3rd ed. New York: McGraw-Hill, 1954.
11. Atomic Energy Commission. The Reactor Handbook, Vol. 2, AECD-3646. May, 1955.
12. Bush, P. D., et al. Engineering Test Reactor Engineering Design and Safeguards Report. IDO-24020. July, 1956.
13. Carter, R. L., et al. "Recent Developments in the Technology of Sodium-Graphite Reactor Materials," Proceedings of the Second United Nations International Conference on the Peaceful Uses of Atomic Energy, Vol. 7, Reactor Technology, Geneva, Switzerland. September 1-13, 1958.
14. Atomic Energy Commission. The Reactor Handbook, Vol. 3, AECD-3647. March, 1955.
15. American Lava Corporation. Al-Si-Mag, Chart No. 591. Chattanooga, undated.
16. Aluminum Company of America. Alcoa Structural Handbook. Pittsburgh: Aluminum Company of America, 1956.
17. Marks, L. S., ed. Mechanical Engineers' Handbook, 5th ed. New York: McGraw-Hill, 1951.

APPENDIX A

DESIGN AND HEAT TRANSFER CALCULATIONS

SUMMARY

FLUX MAXIMUM VALUES (design)	
Neutron, nv:	
10-0.18 Mev	3.7×10^{14}
0.18 Mev-0.17 ev	3.5×10^{14}
Less than 0.17 ev	2.2×10^{14}
Gamma Heating, watts/g:	12
Btu/(hr)(g):	41.0
SAMPLE DESCRIPTION	
Assembly Size:	
Graphite Cylinder	1 inch in diameter 3-7/8 inches long
Weight:	
Sample, g	76.1
Assembly, g/ft	570
HEAT GENERATION	
Graphite Core, Btu/(hr)(ft)	12,100
Total Assembly, Btu/(hr)(ft)	23,400
HEAT FLUX	
Capsule Surface, Btu/(hr)(sq ft)	44,800
COOLANT CONDITIONS	
Water Flow Past Capsule, gpm:	130
Water Velocity Past Capsule, ft/sec:	26
TEMPERATURES	
Capsule Surface Temperature, F	130
Sample Temperature Range, F	800 to 1500
C	400 to 850
GAS ATMOSPHERE	
Helium Pressure, psia at 1000 C	65
MECHANICAL STRENGTH, SAFETY FACTOR	
Collapsing	6

A. COOLANT FLOW

Calculation of Capsule Coolant Conditions

1. Design Information:

Water Temperature	120 F
Pressure Drop Through Core	25 psi
Capsule	2 inch diameter 3003-H14 Aluminum Tubing
Guide Tube	2-1/2 inch diameter Schedule 40 Aluminum Pipe

Dimensions:

Capsule, OD	2.00 inches
Protection Tube, OD	1.100 inches
Guide Tube, ID	2.469 inches
Flow Restricter, ID	2.12 inches
OD	2.437 inches

2. Data for Water at 120 F:

Density, ρ 61.7 lb/cu ft (Ref. 10, p. 484)

3. Pressure Drop, ΔP:

Series of Contractions and Enlargements

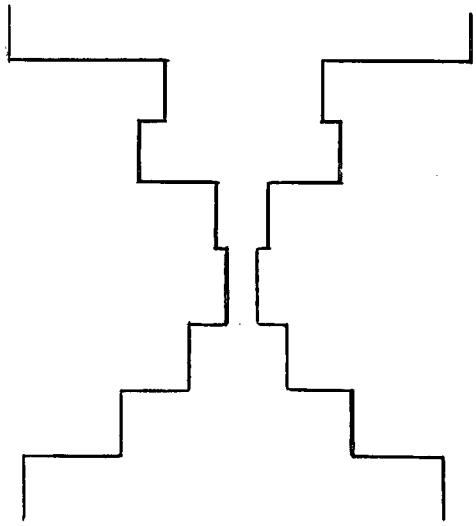

A_1 A_1 - Tank

A_2 A_2 - Holes in Guide Tube

A_3 A_3 - Capsule

A_4 A_4 - Slots in Flow Restrictor

A_5 A_5 - Flow Annulus

A_6 A_6 - Bottom Support Tube

A_7 A_7 - Bottom Support

A_8 A_8 - Tank

Along Capsule

$$\Delta P = \frac{f\, L\, \rho\, V^2}{D_e\, 2\, g_c}$$

$$= \frac{f\, L\, \rho V^2\ [ft^2/sec^2]}{D_e\ (2)\ (32.2)\ [ft/sec^2]} \times \frac{61.7[lb/ft^3]}{144\ [in^2/ft^2]}$$

$$= 0.00665\, \frac{f\, L\, V^2}{D_e}\ psi$$

Contraction

$$\Delta P = \frac{K_c\, V_2^{\,2}}{2\, g_c}$$

$$= 0.00665\, K_c V_2^{\,2}\ psi$$

K_c from Figure 1.5.7 (Ref. 11, p. 67)

Enlargement

$$\Delta P = \frac{K_e\, V_1^{\,2}}{2\, g_c}$$

$$= 0.00665\, K_e\, V_1^{\,2}\ psi$$

K_e from Figure 1.5.6 (Ref. 11, p. 66)

4. Water Velocity, V:

$$V = F[gpm]\ 0.1337\left[\frac{ft^3}{gal}\right] \times \frac{[min]}{60\ [sec]} \times \frac{144\ [in^2]}{[ft^2]} \times \frac{1}{A\ [in^2]}$$

$$= \frac{0.321\ F}{A}\ ft/sec$$

5. Water Flow, F:

Location	Area, in^2	Velocity, ft/sec $\times 10^2 F^{-1}$	Coefficient	Pressure Drop, psi $\times 10^4 F^{-2}$
A_1	Large	0		
			$K_c = 0.40$	1.03
A_2	1.625	19.7		
			$K_e = 0.01$	0.03
A_3	1.646	19.5		6.66
			$K_c = 0.31$	3.65
A_4	0.762	42.1		
			$K_c = 0.10$	1.52
A_5	0.672	47.8		
			$K_e = 0.28$	4.25
A_6	1.455	22.1		
			$K_e = 0.15$	0.49
A_7	2.406	13.3		
			$K_e = 1.0$	1.18
A_8	Large	0		
			Total	18.79

Thus, $0.00188 F^2 = 25$ $F = 130$ gpm

B. CAPSULE TEMPERATURES AND HEAT FLUX

Calculation of the Maximum Can Wall Temperature

1. Coolant Conditions

Water Flow	130 gpm
Velocity Past Capsule	26 ft/sec
Equivalent Diameter	$D_e = 0.469$ in. $= 0.0391$ ft

2. Data for Water at 120 F

Viscosity, μ	1.36 lb/(hr)(ft) (Ref. 10, p. 484)
Thermal Conductivity, k	0.372 Btu/(hr)(ft^2)(°F) per ft (Ref. 10, p. 484)
Heat Capacity, c	1.0 Btu/(lb)(°F) (Ref. 10, p. 462)

3. Water Film Coefficient, h:

$$h = 0.020 \frac{k}{D} \left[N_{RE}\right]^{0.8} \left[N_{PR}\right]^{0.33} \quad \text{(Ref. 12)}$$

Reynolds Number, N_{RE}

$$N_{RE} = \frac{D_e V \rho}{\mu}$$

$$= \frac{0.0391[\text{ft}] \times 26\ [\text{ft/sec}] \times 61.7\ [\text{lb/ft}^3] \times 3600\ [\text{sec/hr}]}{1.36\ [\text{lb/(hr)(ft)}]}$$

$$= 1.66 \times 10^5$$

Prandtl Number, N_{PR}

$$N_{PR} = \frac{c \mu}{k}$$

$$= \frac{1.0[\text{Btu/(lb)(°F)}] \times 1.36[\text{lb/(hr)(ft)}]}{0.372\ [\text{Btu/(hr)(ft)(°F)}]}$$

$$= 3.65$$

$$h = 0.030 \frac{k}{D} (1.66 \times 10^5)^{0.8} (3.65)^{0.33}$$

$$= \frac{0.372\ [\text{Btu/(hr)(ft)(°F)}]}{0.0391\ [\text{ft}]} (0.020)(1.50 \times 10^4)(1.54)$$

$$= 4400\ \text{Btu/(hr)(ft}^2\text{)(°F)}$$

Therefore, the water film coefficient is 4400 Btu/(hr)(ft^2)(°F).

4. Heat Generation

Basis

Sample Length	3.875 inches
Sample Assembly Length	5.25 inches
Maximum Flux, watts/g	12
Btu/(hr)(g)	41.0

Mass

Sample - Graphite	76.1 g	} Assembly Core
Sample Holder - Graphite	53.1 g	
Spacer - Molybdenum	8.8 g	
Ring - Aluminum	13.1 g	
Can - Aluminum	98.2 g	
Total - 5.25-inch section	249.3 g	
per foot	570.0 g	

Assembly Core

$$q_c = \frac{129.2\ [g]}{5.25\ [in]} \times \frac{12\ [in]}{[ft]} \times 41.0 \left[\frac{Btu/hr}{g}\right]$$

$$= 12,100\ Btu/(hr)(ft)$$

Assembly Section

$$q_a = 570 \left[\frac{g}{ft}\right] \times 41.0 \left[\frac{Btu/hr}{g}\right] = 23,400\ Btu/(hr)(ft)$$

5. Heat Flux

$$\frac{q_a}{A} = \frac{23,400\ [Btu/(hr)(ft)]}{(\pi)(2/12)[ft]} = 44,800\ Btu/(hr)(ft^2)$$

6. Film Temperature Drop

$$\Delta T = \frac{q_a}{h\ A}$$

$$= \frac{44,800\ [Btu/(hr)(ft^2)]}{4,400\ [Btu/(hr)(ft^2)(°F)]}$$

$$= 10\ F$$

7. Internal Can Wall Temperature

Temperature Drop Across Can Wall

$$\Delta t = \frac{q\ \ln(D_2/D_1)}{k\ 2\ \pi\ L}$$

For a 5.25-Inch Assembly Section

$$\Delta t = \frac{23,400\ [\text{Btu}/(\text{hr})(\text{ft})]\ (5.25/12)[\text{ft}]\ \ln(2.00/1.87)}{120\ [\text{Btu}/(\text{hr})(\text{ft})(°\text{F})]\ (2)(\pi)(5.25/12)[\text{ft}]}$$

$$= 2\ \text{F}$$

Therefore, the maximum internal can wall temperature is

120 F + 10 F + 2 F = 132 F.

Calculation of the Sample Surface Temperature

1. Basic Data:

Thermal Conductivities		Btu/(hr)(ft^2)(°F)/ft	
Graphite 200-1800 F (Irradiated)		15	(Ref. 13)
Aluminum		128	(Ref. 14, p. 14)
Alundum		0.97	(Ref. 15)
Vitreous Alumina		9.67	(Ref. 15)
Molybdenum		72	(Ref. 14, p. 193)
Helium	200 F	0.0980	(Ref. 11, p. 394)
	500 F	0.112	
	1000 F	0.133	
	1500 F	0.155	
	2000 F	0.172	
	2500 F	0.182	

Emissivities		ϵ	
Aluminum	200 F	0.20	(Ref. 10, p. 476)
Alundum	1800 F	0.40	(Ref. 10, p. 472)
Graphite	1800 F	0.80	(Ref. 10, p. 476)

Assembly Dimensions

Sample - Graphite	1.00 in. diameter × 3-7/8 in. long
Sample Holder - Graphite	1.250 in. OD × 0.750 in. ID × 2 in. long
Centering Disc - Molybdenum	1.800 in. OD × 0.750 in. ID × 0.030 in. thick
Cooling Ring - Aluminum	1.865 in. OD × 1.375 in. ID × 0.313 in. thick
Capsule Shell - Aluminum	2.00 in. OD × 1.87 in. ID × 5.250 in. section

Gamma Heating

Sample Position	Core Elevation, Inches	Watts Per Gram
1	31.1	5.5
2	25.9	7.0
3	20.8	9.5
4	15.6	11.0
5	10.6	10.5
6	5.4	8.0
Core Bottom		

2. Thermal Resistance Calculation:

Total resistance to heat flow, R_T, is formed by parallel combination of the following heat paths

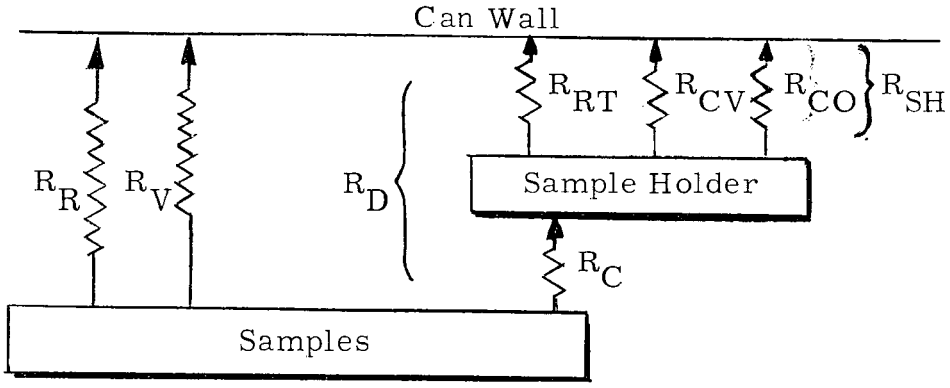

Three parallel paths from sample holder to can wall:

R_{RT} - radiation resistance
R_{CV} - resistance to conduction through helium
R_{CO} - resistance to conduction through molybdenum and aluminum supports
R_{SH} - total resistance from sample holder to can wall

$$R_{SH} = \frac{1}{\frac{1}{R_{RT}} + \frac{1}{R_{CV}} + \frac{1}{R_{CO}}}$$

One series path from sample to can wall through supports

R_C - resistance to conduction through graphite sample holder
R_D - total resistance to conduction through supports

$$R_D = R_C + R_{SH}$$

Three parallel paths from samples to can wall:

R_R - radiation resistance
R_V - resistance to conduction through helium
R_D - resistance to conduction through supports
R_T - total resistance

$$R_T = \frac{1}{\frac{1}{R_R} + \frac{1}{R_V} + \frac{1}{R_D}}$$

Radiation Resistance

Sample to Can Wall, R_R

$$\mathcal{F}_{12} = \frac{1}{\frac{1}{\bar{F}} + \left(\frac{1}{\epsilon_1} - 1\right) + \frac{A_1}{A_2}\left(\frac{1}{\epsilon_2} - 1\right)}$$

$\bar{F}$ = 1 for coaxial cylinders

$$\mathcal{F}_{12} = \frac{1}{\frac{1}{1} + \left(\frac{1}{0.80} - 1\right) + \frac{1.00}{1.87}\left(\frac{1}{0.20} - 1\right)} = 0.295$$

$$h_r = \frac{4 \times 0.173 \times 0.295}{100}\left(\frac{T_{avg}}{100}\right)^3$$

$$= 0.00204\left(\frac{T_{avg}}{100}\right)^3$$

$$R_R = \frac{1}{h_r A}$$

$$A = \frac{3.00 \times (1.00)(\pi)}{(12)(12)} = 0.0654 \text{ ft}^2$$

$$R_R = \frac{1}{0.0654 \times 0.00204 \left(\frac{T_{avg}}{100}\right)^3} = \frac{7500}{\left(\frac{T_{avg}}{100}\right)^3}$$

Sample Holder to Can Wall, R_{RT}

$$\mathcal{F}_{12} = \frac{1}{\frac{1}{1} + \left(\frac{1}{0.80} - 1\right) + \frac{1.25}{1.87}\left(\frac{1}{0.20} - 1\right)} = 0.255$$

$$h_r = \frac{4 \times 0.173 \times 0.255}{100}\left(\frac{T_{avg}}{100}\right)^3 = 0.00177\left(\frac{T_{avg}}{100}\right)^3$$

$$A = \frac{2 \times (1.25)(\pi)}{(12)(12)} = 0.0545 \text{ ft}^2$$

$$R_{RT} = \frac{1}{0.0545 \times 0.00177\left(\frac{T_{avg}}{100}\right)^3} = \frac{10,400}{\left(\frac{T_{avg}}{100}\right)^3}$$

Resistance of Supports, R_C and R_{CO}

Through Sample Holder, R_C

$$R = \frac{\ln\left(D_2/D_1\right)}{(2)(\pi)(L)(k)}$$

$$R_C = \frac{\ln (1.25/0.75)}{(2)(2/12)(15)} = 0.032\,(^\circ\text{F})(\text{hr})/\text{Btu}$$

Through Molybdenum and Aluminum, R_{CO}

Molybdenum Spacer

Effective Heat Transfer Diameters

$$OD = \frac{(1.800 - 0.252) + 1.375}{2} = 1.462 \text{ inches}$$

$$ID = \frac{1.25 + 0.750}{2} = 1.00 \text{ inch}$$

$$R_M = \frac{\ln (1.462/1.00)}{(2)(\pi) \times \frac{0.030}{12} \times 72} = 0.336 \text{ (°F)(hr)/Btu}$$

$$R_{AL} = \frac{\ln (1.865/1.375)}{(2)(\pi) \times \frac{0.313}{12} \times 128} = 0.0147 \text{ (°F)(hr)/Btu}$$

$$R_{CO} = R_M + R_{AL} = 0.351 \text{ (°F)(hr)/Btu}$$

$$\frac{1}{R_{CO}} = 2.85 \text{ Btu/(hr)(°F)}$$

Conduction Through Gas

Helium

$$N_{GR} = \frac{x^3 \rho^2 g \beta \Delta t}{\mu^2}$$

1000 °F 45 psia

$$x^3 = \left(\frac{D_e}{2}\right)^3 = \left(\frac{1.87 - 1.00}{2}\right)^3 = 4.8 \times 10^{-5} \text{ ft}^3$$

$$\rho^2 = (0.0114)^2 = 1.58 \times 10^{-4} (\text{lb/ft}^3)^2$$

$$g = 32.17 \text{ ft/sec}^2$$

$$= 4.19 \times 10^8 \text{ ft/hr}^2$$

$$\beta = \frac{1}{T_{avg} \text{ °R}} = \frac{1}{1026 \text{ °R}}$$

$$\Delta t = 868 \text{ °R}$$

$$\mu^2 = (0.0726)^2 = 5.3 \times 10^{-3} [\text{lb/hr ft}]^2$$

$$N_{GR} = \frac{4.8 \times 10^{-5} [\text{ft}^3] \times 1.58 \times 10^{-4} [\text{lb/ft}^3]^2 \times 4.19 \times 10^8 [\text{ft/hr}^2] \times 868 [\text{°R}]}{1026 [\text{°R}] \times 5.3 \times 10^{-3} [\text{lb/hr ft}]^2}$$

$$= 5.0 \times 10^2$$

Thus $N_{GR} < 2 \times 10^3$ and convection is suppressed so that conduction controls the heat transfer.

$$h_c = \frac{k}{x}$$

$$R = \frac{1}{h_c A} \frac{\ln (D_2/D_1)}{2 k \pi L}$$

From Samples to Wall, R_V

$$R_V = \frac{\ln (1.87/1.00)}{2 k \pi (3.00/12)} = \frac{0.398}{k}$$

From Sample Holder to Wall, R_{CV}

$$R_{CV} = \frac{\ln (1.87/1.25)}{2 k \pi (2/12)} = \frac{0.384}{k}$$

Total Resistance, R_T

$$R_{SH} = \frac{1}{\frac{1}{R_{RT}} + \frac{1}{R_{CO}} + \frac{1}{R_{CV}}}$$

$$R_D = R_{SH} + R_C$$

$$R_T = \frac{1}{\frac{1}{R_D} + \frac{1}{R_R} + \frac{1}{R_V}}$$

TABLE VII

THERMAL RESISTANCES OF AN H-3 CAPSULE

	Resistances (°F)(hr)/Btu											
T_1 °F	$\frac{1}{R_{RT}}$	$\frac{1}{R_{CO}}$	$\frac{1}{R_{CV}}$	$\frac{1}{R_{SH}}$	R_{SH}	R_C	R_D	$\frac{1}{R_D}$	$\frac{1}{R_R}$	$\frac{1}{R_V}$	$\frac{1}{R_T}$	R_T
200	0.0240	2.85	0.255	3.13	0.320	0.032	0.352	2.84	0.033	0.246	3.12	0.320
500	0.0457	2.85	0.292	3.19	0.314	0.032	0.346	2.89	0.063	0.281	3.23	0.310
1000	0.105	2.85	0.346	3.30	0.303	0.032	0.335	2.98	0.146	0.334	3.46	0.289
1500	0.202	2.85	0.403	3.46	0.289	0.032	0.321	3.12	0.280	0.389	3.79	0.264
2000	0.345	2.85	0.446	3.64	0.275	0.032	0.307	3.26	0.478	0.431	4.17	0.240
2500	0.544	2.85	0.474	3.87	0.259	0.032	0.291	3.44	0.752	0.456	4.56	0.215

The data are shown graphically in Figure 22.

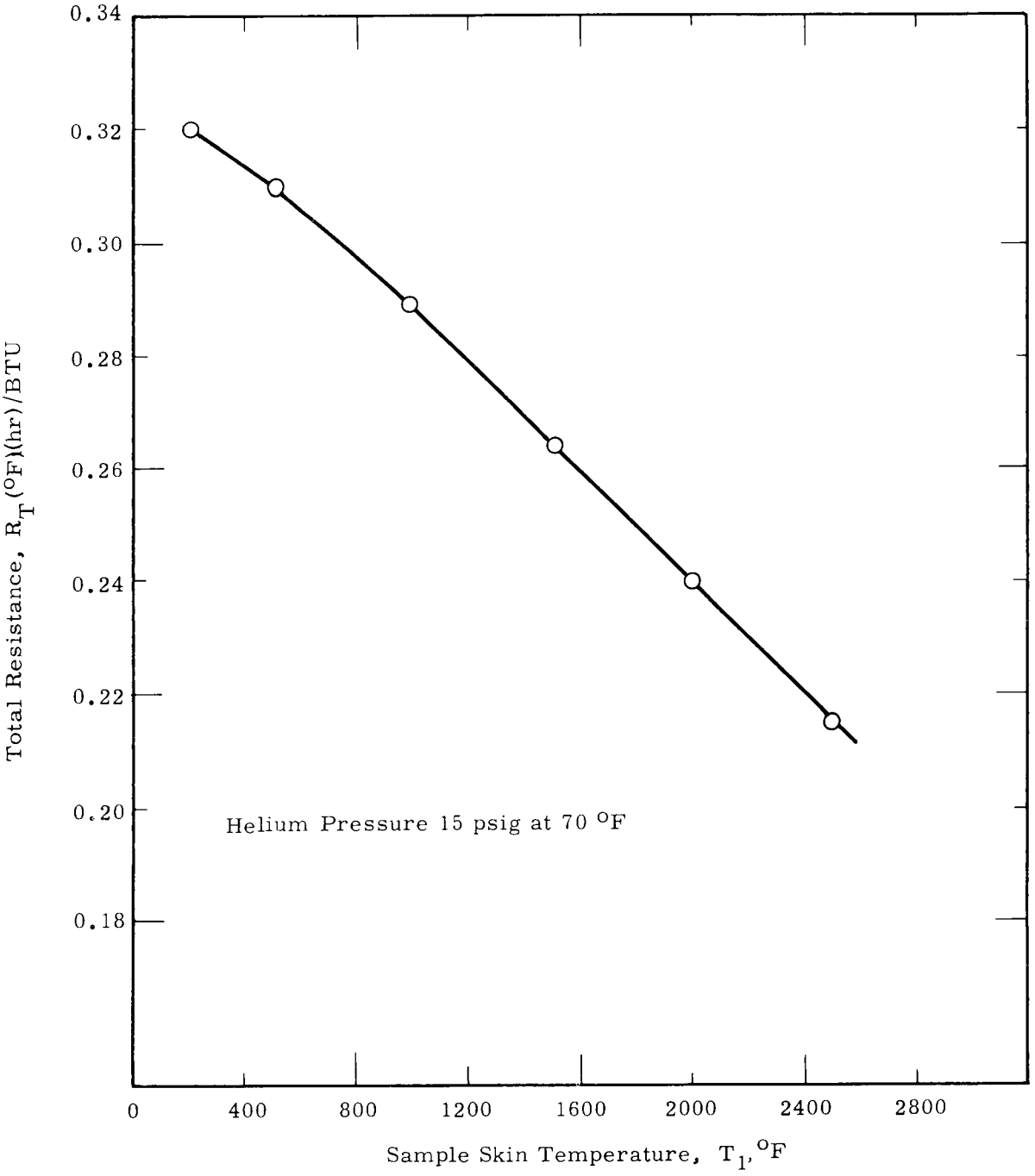

FIGURE 22

Thermal Resistance as a Function of Temperature

AEC-GE RICHLAND, WASH.

Maximum Surface Temperature

Position 1

Heat Input

$$Q_1 = 5.5\ [\text{watts/gram}] \times 129.2\ [\text{grams}] \times 3.42 \left[\frac{\text{Btu/hr}}{\text{watt}}\right]$$

$$= 2430\ \text{Btu/hr}$$

Trial Temperature, 850 F

$$T_1 = 850\ \text{F}, \Delta T = 850 - 132 = 718\ \text{F}$$

$$R_T = 0.295\ (°\text{F})(\text{hr})/\text{Btu from Figure 22}$$

$$Q_2 = \frac{718\ [\text{F}]}{0.295\ [(°\text{F})(\text{hr})/\text{Btu}]} = 2430\ \text{Btu/hr}$$

which satisfies the conditions that $Q_1 = Q_2$ at the temperature that produces a net resistance of the value calculated.

Position 2

Heat Input

$$Q_1 = 7.0 \times 129.2 \times 3.42 = 3100\ \text{Btu/hr}$$

Trial Temperature, 1025 F

$$T_1 = 1025\ \text{F}, \Delta T = 1025 - 132 = 893\ \text{F}$$

$$R_T = 0.288\ (°\text{F})(\text{hr})/\text{Btu}$$

$$Q_2 = \frac{893\ [\text{F}]}{0.288\ [(°\text{F})(\text{hr})/\text{Btu}]} = 3100$$

which satisfies the flux condition.

Position 3

Heat Input

$$Q_1 = 9.5 \times 129.2 \times 3.42 = 4200\ \text{Btu/hr}$$

Trial Temperature, 1290 F

$$T_1 = 1290 \text{ F}, \quad \Delta T = 1290 - 132 = 1158 \text{ F}$$

$$R_T = 0.275 \text{ (°F)(hr)/Btu}$$

$$Q_2 = \frac{1158 \text{ [F]}}{0.275 \text{ [(°F)(hr)/Btu]}} = 4210 \text{ Btu/hr}$$

which satisfies the flux condition.

Position 4

Heat Input

$$Q_1 = 11.0 \times 129.2 \times 3.42 = 4860 \text{ Btu/hr}$$

Trial Temperature, 1430 F

$$T_1 = 1430 \text{ F}, \quad \Delta T = 1430 - 132 = 1298 \text{ F}$$

$$R_T = 0.268 \text{ (°F)(hr)/Btu}$$

$$Q_2 = \frac{1298 \text{ [F]}}{0.268 \text{ [(°F)(hr)/Btu]}} = 4850 \text{ Btu/hr}$$

which satisfies the flux condition.

Position 5

Heat Input

$$Q_1 = 10.5 \times 129.2 \times 3.42 = 4650 \text{ Btu/hr}$$

Trial Temperature, 1380 F

$$T_1 = 1380 \text{ F}, \quad \Delta T = 1380 - 132 = 1248 \text{ F}$$

$$R_T = 0.270 \text{ (°F)(hr)/Btu}$$

$$Q_2 = \frac{1248 \text{ [F]}}{0.270 \text{ [(°F)(hr)/Btu]}} = 4650 \text{ Btu/hr}$$

which satisfies the flux condition.

Position 6

Heat Input

$$Q_1 = 8.0 \times 129.2 \times 3.42 = 3530 \text{ Btu/hr}$$

Trial Temperature, 1130 F

$$T_1 = 1130 \text{ F}, \quad \Delta T = 1130 - 132 = 998 \text{ F}$$

$$R_T = 0.283 \text{ (°F)(hr)/Btu}$$

$$Q_2 = \frac{998 \text{ [F]}}{0.283 \text{ [(°F)(hr)/Btu]}} = 3530 \text{ Btu/hr}$$

which satisfies the flux condition.

Calculation of Maximum Sample Temperature

Temperature Drop in Graphite

$$\Delta T = \frac{q_1}{4 \pi k L}$$

Position 1

$$\Delta T = \frac{5.5 \text{ [watts/gram]} \times 76.1 \text{ [grams]} \times 3.42 \left[\frac{\text{Btu/hr}}{\text{watt}}\right]}{4 \times \pi \times 15 \text{ [Btu/(hr)(ft}^2\text{)(°F)/ft]} \times (5.25/12) \text{ [ft]}} = 18 \text{ F}$$

Maximum Sample Temperature 850 F + 18 F = 868 F

465 C

Position 2

$$\Delta T = \frac{7.0 \times 76.1 \times 3.42}{4 \times \pi \times 15 \times (5.25/12)} = 24 \text{ F}$$

Maximum Sample Temperature 1025 F + 24 F = 1049 F

565 C

Position 3

$$\Delta T = \frac{9.5 \times 76.1 \times 3.42}{4 \times \pi \times 15 \times (5.25/12)} = 30 \text{ F}$$

Maximum Sample Temperature 1290 F + 30 F = 1320 F

715 C

Position 4

$$\Delta T = \frac{11.0 \times 76.1 \times 3.42}{4 \times \pi \times 15 \times (5.25/12)} = 35 \text{ F}$$

Maximum Sample Temperature 1430 F + 35 F = 1465 F
800 C

Position 5

$$\Delta T = \frac{10.5 \times 76.1 \times 3.42}{4 \times \pi \times 15 \times (5.25/12)} = 34 \text{ F}$$

Maximum Sample Temperature 1380 F + 34 F = 1414 F
770 C

Position 6

$$\Delta T = \frac{8.0 \times 76.1 \times 3.42}{4 \times \pi \times 15 \times (5.25/12)} = 25 \text{ F}$$

Maximum Sample Temperature 1130 F + 25 F = 1155 F
625 C

C. MECHANICAL STRENGTH OF CAPSULE

Collapsing Pressure, Ignoring the Support of the Cooling Rings

Shell	2 in. OD × 0.065 in. wall	
Material	3003-H14 Aluminum	
Minimum Mechanical Properties		
Yield Strength - Compression	15,000 psi	(Ref. 16, p. 55)
Rating for Temperature, YS	100% at 75 °F	(Ref. 16, p. 70)
	89% at 212 °F	

$$P = 2 S_c \left[\frac{t}{D} - \left(\frac{t}{D}\right)^2\right] \text{ when } \frac{t}{D} > 0.03 \qquad \text{(Ref. 17, p. 422)}$$

$$P = 2 \times 15,000 \times 0.89 \left[(0.0325) - (0.0325)^2\right]$$

$$= 840 \text{ psia}$$

Reactor Pressure	140 psia
Safety Factor	$\frac{840}{140} = 6.0$

APPENDIX B

DETERMINATION OF EXPOSURE

A. EXPERIMENTAL PROCEDURE

Three types of flux monitor foils were inserted into each cooling ring prior to the irradiation of the H-3-1 capsule. These were nickel wire (0.020-inch diameter), iron wire (0.063-inch diameter), and 0.1 per cent cobalt in aluminum wire (0.040-inch diameter). Approximate weights were 0.15, 0.85, and 0.09 gram, respectively. Upon completion of the four cycles of irradiation these were removed, weighed, and the following gamma energies counted on a 256 channel analyzer:

Ni^{58} (n, p) Co^{58}	0.82 Mev gamma emission
Fe^{54} (n, p) Mn^{54}	0.84 Mev gamma emission
Co^{59} (n, γ) Co^{60}	1.31 Mev gamma emission

The fast flux distribution was based on the results from the nickel and iron monitors. The nickel foils were corrected for cobalt burnout. A value of 3750 barns was used for the thermal absorption cross section of Co^{58} as derived for the H-1 experiment (see HW-64286, Appendix IV). Analysis of the supposedly pure iron wire was not completed until after the irradiation had begun. The results indicated the wire was only 72 per cent iron, with a high percentage of nickel impurity. The Mn^{54} formed was separated by ion exchange from the iron foil before it was counted; however, the results may be in error due to Co^{58} formed from the nickel impurity.

B. FORMULAS

Fast Flux, Ni^{58} (n, p) Co^{58}

The number of Co^{58} atoms, n, present at any time, t, is found by integration of the following differential equation:

$\frac{dn}{dt}$ = number formed - number disintegrated - number burned out

$\frac{dn}{dt} = \sigma_{act} N \varphi_f - \lambda n - \sigma_{abs} \varphi_{th} n$

n = number of Co^{58} atoms per milligram foil

N = Number of Ni^{58} atoms per milligram foil

t = time

σ_{act} = activation cross section, Ni^{58}

φ_f = average fast flux

λ = disintegration constant for Co^{58}

σ_{abs} = absorption cross section, Co^{58}

φ_{th} = average thermal flux

Assuming φ_f to be a square wave with a magnitude equal to a constant during each operating period and equal to zero during each shutdown one can obtain the following:

$$\varphi_f t_{op} = \frac{A}{\sigma_{act} N} \left[(\lambda - \sigma_{abs}\varphi_{th})t_{op}\right] \left[\sum_{j=1}^{m} \frac{1 - e^{-(\lambda + \sigma_{abs}\varphi_{th})t_{ij}}}{\left(e^{\lambda t_{sj}}\right)\left(e^{\lambda + \sigma_{abs}\varphi_{th} t_{ij}} + 1\right)\left(e^{\lambda t_{sj}} + 1\right)}\right]^{-1}$$

where:

$t_{op} = \sum_{j=1}^{m} t_{ij}$ is the total operating time

j = 1, 2, 3 $\cdots$ m each operating time

t_{ij} = operating time for the j^{th} operating period

t_{sj} = time of the shutdown following the j^{th} operating period

t_{oj} = time from the end of the end of the j^{th} operating period to the date of foil counting

Constants

$$\lambda = \frac{0.693}{71.3 \text{ days}} = 0.972 \times 10^{-2} \text{ day}^{-1} = 1.12 \times 10^{-7} \text{ sec}^{-1}$$

$N = 6.94 \times 10^{18}$ atoms Ni^{58} per mg.

σ_{act} = 91 millibarns over the entire fission (Watt) spectrum

For E > 2 Mev

$$\sigma_{act} = \frac{91}{0.397} = 229 \text{ mb}$$

For GETR Spectrum - GNU II Calculations

E > 2 Mev

σ_{act} = 229 mb (Implies agreement with Watt spectrum in excess of 2 Mev)

E > 1 Mev

$\sigma_{act} = 229 \times 0.524 = 120$ mb

$$\frac{1}{\sigma_{act} N} = 1.07 \times 10^{13} \quad \text{for E > 1 Mev}$$

σ_{abs} = 3750 barns (Ref. 5)

$$\sigma_{abs}\varphi_{th} = 3.24 \times 10^{-16} \varphi_{th} \text{ cm}^2 \text{ sec/day}$$

Ni^{58} basic equation

$$\varphi_f t_{op} = \left[1.07 \times 10^{13} A \; zt_{op}\right] \left[\sum_{j=1}^{m} \frac{1 - e^{-zt_{ij}}}{\left(e^{0.972 \times 10^{-2} t_{sj}}\right)\left(e^{zt_{ij}} + 1\right)\left(e^{0.972 \times 10^{-2} t_{sj}} + 1\right)\ldots}\right]^{-1}$$

$$z = (0.972 \times 10^{-2} + 3.24 \times 10^{-16} \varphi_{th})$$

where

A = specific activity of foil at time of counting.

Fast Flux, Fe^{54} (n, p) Mn^{54}

The number of Mn^{54} atoms, n, present at any time, t, is found by integration of the following differential equation:

$\frac{dn}{dt}$ = number formed - number disintegrated

$\frac{dn}{dt} = \sigma_{act} N \varphi_f - \lambda n$

n = number of Mn^{54} atoms per milligram foil

N = number Fe^{54} atoms per milligram foil

t = time

σ_{act} = activation cross section, Fe^{54}

φ_f = average fast flux

λ = disintegration constant for Mn^{54}

Constants

$\lambda = \frac{0.693}{291 \text{ days}} = 2.38 \times 10^{-3} \text{ day}^{-1} = 2.75 \times 10^{-8} \text{ sec}^{-1}$

$N = 4.60 \times 10^{17}$ atoms Fe^{54} per mg.

σ_{act} = 53 mb over the entire fission spectrum

For GETR spectrum and E > 1 Mev

$\sigma_{act} = 69.9$ mb

$$\frac{1}{\sigma_{act} N \lambda} = 1.13 \times 10^{15} \text{ for } E > 1 \text{ Mev}$$

Therefore, the basic equation derived in the same manner as the one in Section A with no $\sigma_{abs}\varphi_{th}$ term, becomes:

$$\varphi_f t_{op} = 1.13 \times 10^{15} A \left[2.38 \times 10^{-3} t_{op}\right] \left[\sum_{j=1}^{m} \frac{1 - e^{-\left(2.38 \times 10^{-3} t_{ij}\right)}}{\left(e^{2.38 \times 10^{-3} t_{oj}}\right)}\right]^{-1}$$

Thermal Flux, Co^{59} (n, γ) Co^{60}

The number of Co^{60} atoms, n, present at any time, t, is found by integration of the following differential equation:

$\frac{dn}{dt}$ = number formed - number disintegrated

$\frac{dn}{dt} = \sigma_{act} N \varphi_{th} - \lambda n$

n = number of Co^{60} atoms per milligram foil

N = number of Co^{59} atoms per milligram foil

t = time

σ_{act} = activation cross section Co^{59}

φ_{th} = average thermal (cobalt) flux

λ = disintegration constant for Co^{60}

Constants

$\lambda = \frac{0.693}{5.23 \text{ years}} = 3.61 \text{ day}^{-1} = 4.18 \text{ sec}^{-1}$

$N = 1.022 \times 10^{16}$ atoms Co^{59} per mg

$\sigma_{act} = 36$ barns

$\frac{1}{\lambda N \sigma_{act}} = 6.50 \times 10^{14}$

Due to the relatively long half-life of the Co^{60} the t_{ij} terms may be summed to a t_i term and the basic equation becomes:

$$\varphi_{th} t_{op} = 6.50 \times 10^{14} A \left[3.61 \times 10^{-4} t_{op}\right] \left[\frac{e^{3.61 \times 10^{-4} t_o}}{1 - e^{-\left(3.61 \times 10^{-4} t_i\right)}}\right]$$

TABLE VIII

SUMMARY OF CYCLE DATA, H-3-1

Cycle	t_i	t_{sj}	t_{oj}
13	23.7	8.2	153.0
14	24.9	23.4	119.9
15	12.6	6.8	83.9
16	29.1		48.0
	t_{op} = 90.3		

TABLE IX

EXPERIMENTALLY DERIVED EXPOSURE, H-3-1

Cooling Ring Number	Core Elevation, Inches	Exposure (Cycles 13-16)					
		Thermal		Fast			
		Co^{59} Foil		Ni^{58} Foil		Fe^{54} Foil	
		A dis/sec mg, $\times 10^{-6}$	nvt, $\times 10^{-21}$	A dis/sec mg, $\times 10^{-6}$	nvt, $\times 10^{-21}$	A dis/sec mg, $\times 10^{-6}$	nvt, $\times 10^{-21}$
1	33.5	0.683	0.464	5.37	0.283	0.295	0.513
2	28.4			8.20	0.720		
3	23.3	2.09	1.42	8.66	0.948	0.655	1.14
4	18.1	2.47	1.68	9.41	1.18	0.825	1.43
5	13.0	2.85	1.94	9.11	1.29	1.05	1.83
6	7.9	2.27	1.54	8.96	1.04	0.863	1.50
7	2.8	1.72	1.17	7.06	0.664	0.459	0.799
Core Bottom	0						

INTERNAL DISTRIBUTION

Copy Number

1	F. W. Albaugh - H. M. Parker
2	D. E. Baker
3	R. W. Benoliel
4	J. H. Brown
5	S. H. Bush
6	D. H. Curtiss
7	R. E. Dahl
8 - 17	J. M. Davidson
18 - 58	D. R. de Halas
59	R. L. Dickeman
60	R. L. Dillon
61	J. E. Faulkner
62	J. F. Fletcher
63	J. C. Fox
64 - 73	J. W. Helm
74	F. D. Hobbs
75	J. L. Jackson
76	G. A. Last
77	C. E. Love
78	D. B. Lovett
79	J. E. Minor
80	W. C. Morgan - R. D. Gibperson
81	I. T. Myers
82	R. Neidner
83	R. E. Nightingale
84	B. A. Ryan
85	F. W. Woodfield
86	R. E. Woodley
87	E. M. Woodruff
88	H. H. Yoshikawa
89 - 110	Extra
111	300 Files
112	Record Center
113 - 116	GE Technical Data Center, Schenectady

EXTERNAL DISTRIBUTION (Special)

Number of Copies

1 Argonne National Laboratory
Attn: R. M. Adams

1 Brookhaven National Laboratory
Attn: D. H. Gurinsky

2 Division of Reactor Development
Attn: R. E. Pahler
I. F. Zartman

2 General Atomic Division
Attn: R. B. Duffield
R. A. Meyer

2 General Electric Company, Vallecitos Atomic Laboratory
Attn: L. P. Bupp
E W. O'Rorke

1 General Electric Research Laboratories
Attn: E. R. Stover
P. O. Box 1088, Schenectady

1 General Nuclear Engineering Corporation
Attn: W. A. Maxwell

1 Great Lakes Carbon Corporation
Attn: L. H. Juel, Electrode Division
Research and Development Department
P. O. Box 637, Niagara Falls, New York

1 HOO - Technical Information Library

2 Attn: J. M. Musser
R L. Plum

1 Marquardt Corporation
Attn: D. W. Bareis

1 National Carbon Company
Attn: W. P. Eatherly, Carbon Division
P. O. Box 6116, Cleveland 1, Ohio

3 Oak Ridge National Laboratory (Y-12)
Attn: F. L. Carlsen
R. A. Charpie
C. A Preskitt

2 Oak Ridge Operations Office
Attn: W. J Larkin
D. F. Cope

1 Speer Carbon Company
Attn: W E. Parker
Research and Development Laboratories
Packard Road & 47th Street, Niagara Falls

1 Wright Air Development Division
Attn: R H. Wilson (Capt.)

EXTERNAL DISTRIBUTION

Number of Copies	
3	Aberdeen Proving Ground
1	Aerojet-General Corporation
1	Aerojet-General Nucleonics
1	Aeroprojects Incorporated
2	ANP Project Office, Convair, Fort Worth
1	Alco Products, Inc.
1	Allis-Chalmers Manufacturing Company
1	Allis-Chalmers Manufacturing Company, Washington
1	Allison Division - GMC
10	Argonne National Laboratory
1	Armour Research Foundation
1	Army Ballistic Missile Agency
1	AEC Scientific Representative, Belgium
1	AEC Scientific Representative, France
1	AEC Scientific Representative, Japan
3	Atomic Energy Commission, Washington
4	Atomic Energy of Canada Limited
4	Atomics International
4	Babcock and Wilcox Company
2	Battelle Memorial Institute
1	Beryllium Corporation
1	Bridgeport Brass Company
1	Bridgeport Brass Company, Adrian
2	Brookhaven National Laboratory
1	Brush Beryllium Company
1	Bureau of Mines, Albany
1	Bureau of Ships (Code 1500)
1	Carborundum Company
3	Chicago Operations Office
1	Chicago Patent Group
1	Clevite Corporation
1	Combustion Engineering, Inc.
1	Combustion Engineering, Inc. (NRD)
1	Convair-General Dynamics Corporation, San Diego
1	Defense Research Member
1	Denver Research Institute
2	Department of the Army, G-2
1	Dow Chemical Company (Rocky Flats)
4	duPont Company, Aiken
1	duPont Company, Wilmington
1	Frankford Arsenal

EXTERNAL DISTRIBUTION (Contd.)

Number of Copies	
1	Franklin Institute of Pennsylvania
2	General Atomic Division
2	General Electric Company (ANPD)
1	General Electric Company, St. Petersburg
1	General Nuclear Engineering Corporation
1	Glasstone, Samuel
1	Goodyear Atomic Corporation
2	Iowa State University
2	Jet Propulsion Laboratory
1	Johns Hopkins University (ORO)
3	Knolls Atomic Power Laboratory
3	Los Alamos Scientific Laboratory
1	Los Alamos Scientific Laboratory (Sesonske)
1	M & C Nuclear, Inc.
1	Mallinckrodt Chemical Works
1	Maritime Administration
1	Martin Company
1	Mound Laboratory
1	NASA Lewis Research Center
2	National Bureau of Standards
1	National Bureau of Standards (Library)
1	National Carbon Company
2	National Lead Company of Ohio
3	Naval Research Laboratory
1	New Brunswick Area Office
1	New York Operations Office
1	Northern Research and Engineering Corporation
1	Nuclear Development Corporation of America
1	Nuclear Materials and Equipment Corporation
1	Nuclear Metals, Inc.
1	Oak Ridge Institute of Nuclear Studies
2	Office of Naval Research
1	Office of Naval Research (Code 422)
1	Olin Mathieson Chemical Corporation
1	Ordnance Materials Research Office
1	Ordnance Tank-Automotive Command
1	Patent Branch, Washington
4	Phillips Petroleum Company (NRTS)
1	Picatinny Arsenal
1	Power Reactor Development Company
3	Pratt and Whitney Aircraft Division
1	Rensselaer Polytechnic Institute
2	Sandia Corporation, Albuquerque
1	Sandia Corporation, Livermore

EXTERNAL DISTRIBUTION (Contd.)

Number of Copies	
1	Stevens Institute of Technology (Comstock)
1	Sylvania Electric Products, Inc.
1	Technical Research Group
1	Tennessee Valley Authority
2	Union Carbide Nuclear Company (ORGDP)
5	Union Carbide Nuclear Company (ORNL)
1	Union Carbide Nuclear Company (Paducah Plant)
1	USAF Project RAND
1	U. S. Geological Survey, Denver
1	U. S. Geological Survey, Menlo Park
1	U. S. Geological Survey, Washington
1	U. S. Naval Postgraduate School
1	U. S. Patent Office
2	University of California, Berkeley
2	University of California, Livermore
1	University of Puerto Rico
1	Watertown Arsenal
4	Westinghouse Bettis Atomic Power Laboratory
1	Westinghouse Electric Corporation
8	Wright Air Development Division
1	Yankee Atomic Electric Company
325	Division of Technical Information Extension
75	Office of Technical Services, Washington